

# Green synthesis of nickel oxide nanoparticles using plant extracts: an overview of their antibacterial, catalytic, and photocatalytic efficiency in the degradation of organic pollutants

Farzaneh Moradnia<sup>1</sup> , Saeid Taghavi Fardood<sup>2,\*</sup> , Armin Zarei<sup>1</sup> ,  
Siamak Heidarzadeh<sup>3</sup> , Ali Ramazani<sup>1</sup> , Mika Sillanpää<sup>4,5,\*</sup> 

<sup>1</sup>Department of Chemistry, Faculty of Science, University of Zanjan, Zanjan, Iran.

<sup>2</sup>Department of Chemistry, Faculty of Science, Ilam University, Ilam, Iran.

<sup>3</sup>Department of Microbiology and Virology, School of Medicine, Zanjan University of Medical Sciences, Zanjan, Iran.

<sup>4</sup>Department of Chemical Engineering, School of Mining, Metallurgy and Chemical Engineering, University of Johannesburg, South Africa.

<sup>5</sup>Department of Civil Engineering, University Centre for Research & Development, Chandigarh University, Gharuan, Mohali, Punjab, India.

\*Corresponding authors: Saeid Taghavi Fardood: [s.taghavi@ilam.ac.ir](mailto:s.taghavi@ilam.ac.ir), [saeidt64@gmail.com](mailto:saeidt64@gmail.com)  
Mika Sillanpää: [mikaesillanpaa@gmail.com](mailto:mikaesillanpaa@gmail.com)

## Review Paper

Received:  
23 December 2023  
Revised:  
9 February 2024  
Accepted:  
5 March 2024  
Published online:  
20 March 2024

© The Author(s) 2024

## Abstract:

In the past decade, numerous longitudinal studies have explored green chemistry and its applications in nanoparticle synthesis due to the toxicity associated with traditional methods. Among the various techniques for nanoparticle synthesis, the use of plant extracts in green synthesis has recently gained significant popularity. Green methods are particularly suitable for large-scale nanoparticle synthesis, offering faster preparation rates compared to microorganisms and the ability to produce nanoparticles in diverse sizes and shapes. Nickel oxide nanoparticles (NiO NPs) have been extensively utilized in catalysis, photocatalysis, optics, magnetism, and antibacterial applications. This review focuses on the preparation of NiO NPs using plant extracts, emphasizing their advantageous features such as the absence of contaminant release, environmental friendliness, and cost-effectiveness. Additionally, we delve into the catalytic, photocatalytic, and antibacterial applications of NiO NPs.

**Keywords:** Nickel oxide; Green synthesis; Catalytic activity; Antibacterial activity; Photocatalytic ability

## 1. Introduction

Nanotechnology is ascribed as a novel branch of science related to the synthesis of NPs and their utilizations in a wide range of areas such as health, food, space, environmental, and chemical industries, so the demand for eco-friendly and biodegradable methods for the synthesis of nanoparticles is indisputable [1–14]. Nanoparticles are of important interest owing to their very small size and large surface-to-volume

ratio [15–20]. Nanoparticles are particles in the size range of 1–100 nm, and materials at the nanometer sizing represent different properties to those of bulk materials and even the isolated atom. Nanomaterials indicate fortified features such as high catalytic reactivity, thermal conductivity, and chemical steadiness [21–24]. Metal NPs and metal oxide NPs have lately received considerable attention among all the other nanomaterials due to their outstanding properties [25–31]. Generally, there are two approaches for the synthe-

sis of NPs: Bottom-up and top-down (Fig. 1). The former way of NPs synthesis involves the arrangement of smaller molecules atom-by-atom into more complex assemblies and the latter way needs bulk material. In this way, macroscopic particles are first prepared and then they are turned into nanosized materials through a process named plastic deformation. This method is less likely to be applied on a large scale as it is less cost-effective [33–36]. One of the most popular and usual techniques for the preparation of nano substances, which engaged in the top-down method, could be Interferometric Litho- graphic (IL) [37–40]. In the mentioned technique, the self-assembling of the minimized particles plays a vital role in the synthesis of nanomaterials. It is more likely to be an efficient and cost-effective approach [41–43].

In the applied physical procedures for the synthesis of nanoparticles are physical factors needed in the creation of stable and well-structured nano-based materials. The colloidal dispersion method is the best example. The other physical techniques are vapor condensation, amorphous crystallization, and physical fragmentation. Nanoparticle synthesis is gone through physical, chemical, and environment-friendly processes [44–47]. The physical methods are less cost-efficient because of using utilizing expensive facilities, and requiring high temperature and pressure. However, chemical approaches for NPs synthesis, such as chemical microemulsion, wet chemical, direct precipitation and etc. [48–55], involve toxic chemicals that could pose a threat for the environment and people who are

in touch with them. Although a considerable number of studies focused on NPs synthesis from chemical and physical approaches, some terrible side effects of the mentioned two approaches, such as using noxious and carcinogenic chemicals, high vacuum usage needed, and less cost-efficacy, have been reported. [56–61] Therefore, it is undeniable that a cost-efficient and green method is required for the preparation of NPs [62–72]. A green method for the synthesis of NPs could be plant extract usage. This method possesses conving advantages such as cost-efficiency, safety, simple usage, and non-poison [73–75]. Thus, in this review, we have focused on NiO NPs synthesis by means of plant extract usage.

### 1.1 Nickel oxide nanoparticles

NiO NPs stand as one of the most abundant metal oxides on Earth. In the past decade, numerous studies have been conducted to synthesize NiO NPs due to their diverse applications in fields such as electronics, optics, and biomedical systems [76–81]. The preparation of metallic oxides, like  $\text{TiO}_2$ ,  $\text{CuO}$ ,  $\text{ZnO}$ , and  $\text{NiO}$ , has become one of the important subjects in recent studies [82–89]. Among all the mentioned inorganic metal oxides, the NiO NPs have been especially interesting among scientists because these nanoparticles are cost-efficient, easy to prepare, and safe [90]. A. Angel Ezhilarasi et al. presented the NiO NPs by means of the Aegle marmelos plant to treat hazardous diseases in India. High-resolution transmission electron microscopy (HR-TEM) and High-resolution scanning electron microscopy (HR-SEM) analysis indicated the average size of NPs between 8-10

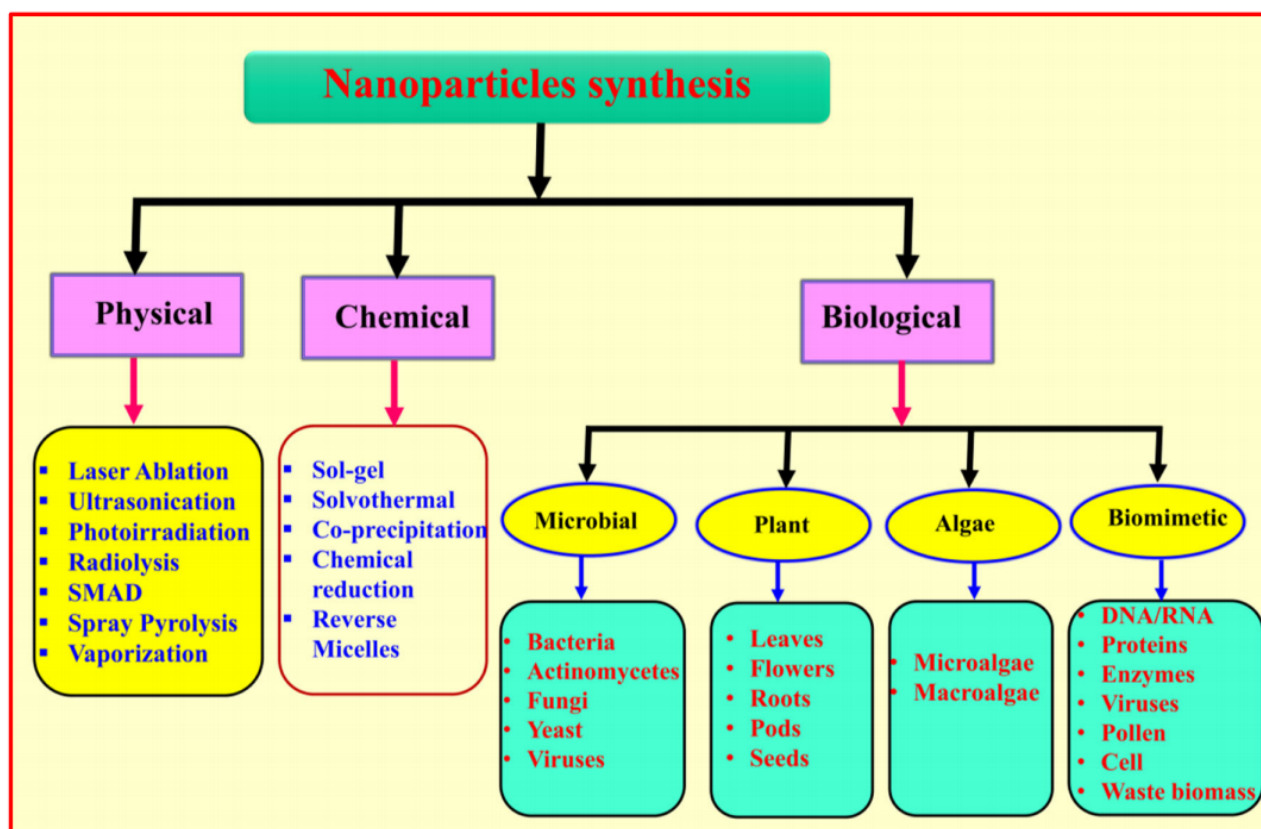
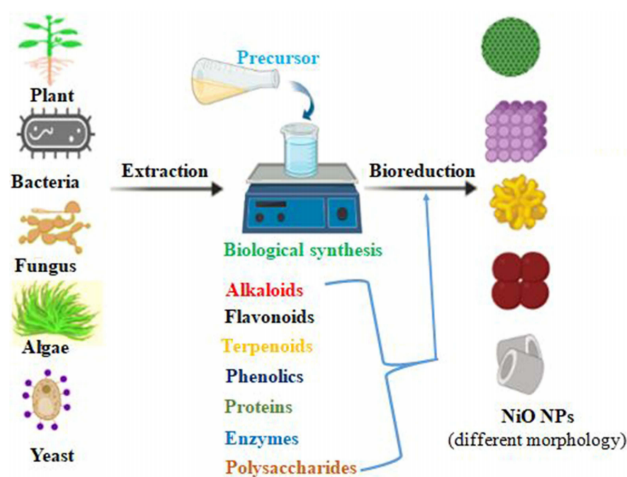


Figure 1. Various methods for the nanoparticle synthesis [32].

nm and the spherical shape of NPs. The band gap of NPs was at 3.5 eV which shows that NiO NPs are active in the visible area, so this is a priceless benefit in comparison to the other photocatalysts like TiO<sub>2</sub> [91]. Diallo et al. reported the NiO NPs synthesis by using *Aspalathus linearis*. In this research, the optical, structural, and photocatalytic activity of the NPs have been considered. The optical analysis showed that NiO NPs had absorption in UV-visible (518.98 nm), in which the more the temperature increased, the less absorption was observed. For example, the bandgap energies fell to below 4 eV when the sample was heated to around 300-400 °C. Furthermore, the final results depicted that NiO NPs have noticeable photocatalytic activity for the degradation of methylene blue [92].

## 1.2 Eco-friendly synthesis the NiO NPs

Recently, researchers have shown an increased interest in nanoparticles synthesis using microorganisms. The advantages of such a method far outweigh the disadvantages. Some [93]. merits of this approach are its cost-efficiency, safety, and being ecologically-friendly [63, 95, 96]. Green synthesis is an approach in which the NPs are produced using plants, bacteria, fungi, algae, etc. [63, 65, 97–99]. Ayesha Mariam et al. synthesized NiO NPs using a billing approach by means of *Azadirachta indica* and *Psidium guajava* with the aim of considering the anti-cancer activities of these NPs. They figured out that the NiO NPs were spherical with a size range of 17-70 nm [100]. B.T. Sone et al. prepared NiO nanopowders by the use of a green approach of aqueous extracts usage from the red flowers of the plant. Callistemon Viminal's X-ray diffraction analysis delineated the average size of NPs to be 20-35 nm with a crystalline shape. The band gap of these NPs was 3.35 eV. Initially controlled redox processes at ambient temperature were proved by electrochemical impedance spectroscopy. This research finally suggested that plant extract is an eco-friendly, safe, harmless, and economical friendly candidate for NiO NPs preparation which could be utilized in energy storage applications [101].



**Figure 2.** Some examples of the nanoparticle synthesis using plant extracts [94].

## 2. Green synthesis and different applications of NiO NPs

### 2.1 Green synthesis of NiO NPs using plant extract

Several parts of the plant like leaf, stem, root, fruit, and seed have been applied for the NPs preparation. Figure 2 depicts a number of nanoparticle synthesis using plant extracts, and Figure 3 showcases synthetic methods of NPs along with their characterizations and applications. NPs synthesis by plant extracts usage also has some merits such as lowcost, biodegradability, being green, lack of intermediate base groups needed and costly equipment usage required, less time-consuming, and it results in products with lesser impurities [102]. One of the most applicable NPs synthesis methods is the NPs fabrication with plant sources because this way leads to nano-based materials with a variety in shape and size [103]. A useful approach in terms of NiO NPs synthesis is a process in which leaves or flowers are added at a basic pH of 12. After shaking the mixture for about 10 min and putting it in a hot air oven as long as 90 min, the mixture color shifted from light to dark green as the reduction process supplemented. Finally, NiO NPs dried and stored for the following usage. The final results of the research clearly showed that NiO NPs, which have been synthesized by using a synthetic nature-friendly method of *Calotropis gigantea* leave usage, have a significant antibiotic potential against *Escherichia coli* and *Bacillus subtilis*. Furthermore, NiO NPs are a convenient choice in a variety of applications because of their proper features such as their magnetic and electrical features. P. Kganyago et al. have recently investigated the innovative and green synthesis of NiO NPs by the use of *Monsonia Burkenea*'s leaves. XRD and HR-TEM analysis proved the preparation of NiO NPs with a 20 nm average size in a spherical shape. The final findings of the research revealed that the NPs have an anti-bacterial property against gram-negative strains, such as *E.*

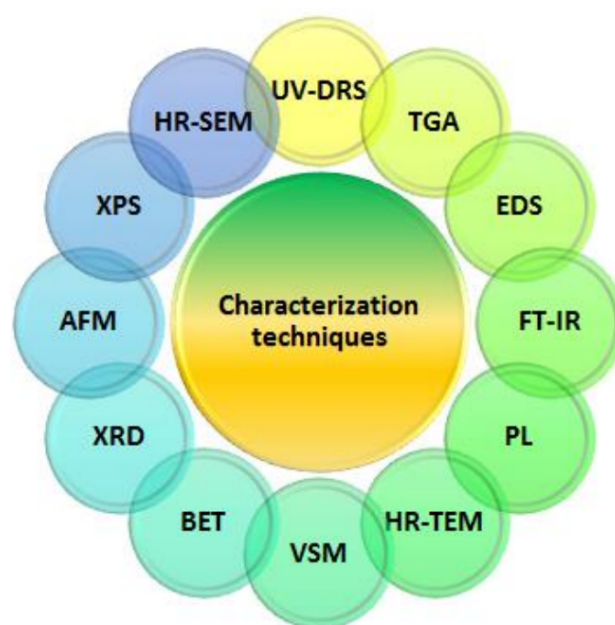


**Figure 3.** Characterization of nanoparticles [104].



*coli* and *Pseudomonas aeruginosa*. The researchers also found that although these NiO NPs are less likely to have a very positive proliferation impact on carcinogenic cells, they could be preferably utilized as drug carriers for cancer treatment in the human body [106]. Ali Talha Khalil et al. prepared the NiO NPs by using sageretia tea (*Osbeckia*) leaves and considered their biological effects. The size of NPs observed by XRD and HR-SEM/TEM analysis was 18 nm and their shape was also spherical. This study has investigated the effects of these NPs on six various gram-positive and gram-negative bacterial strains and finding their toxicity, biocompatibility, antioxidant, and enzyme inhibition features. The results showed that NiO NPs revealed improved antibacterial activities and moderate antioxidant properties. The synthesized NiO NPs also indicated modest enzyme inhibition activities and relatively non-toxicity to human cells [107]. To determine the supercapacitor electrodes applications, Manab Kundu et al. prepared NiO NPs by a green and novel approach to *Hydrangea paniculata* flower extracts usage. The average size of the NPs was 33 nm. The electrode-based NPs depicted high capacitance, and interestingly, the NiO NPs electrodes showed remarkable cycling stability. The mentioned excellent electrochemical proficiency was related to the nano-scale of particles, which eases migration over the rapid charge-discharge procedure, reduces the diffusion path length of ions and electrons and finally enhances the efficient electrochemical application of electroactive material [108].

Singh et al. present the structural and crystallinity information of NiO NPs, as depicted in Fig. 4a. The XRD pattern confirms NiO nanoparticle formation, displaying intense reflection peaks at  $2\theta = 37.3^\circ$ ,  $43.3^\circ$ ,  $62.9^\circ$ ,  $75.6^\circ$ , and  $79.6^\circ$ . The pattern aligns with JCPDS card number 47-1049, indicating a face-centered cubic structure with an average crystallite size of 27.7 nm. BET analysis in Fig. 4b reveals a specific surface area of  $16.71 \text{ m}^2 \text{ g}^{-1}$ , an average pore size of 1.2 nm, and a total pore volume of  $0.32 \text{ cm}^3 \text{ g}^{-1}$ , suggesting mesoporous characteristics with a uniform pore size distribution [105].

Subsequently, Singh et al. utilized HRTEM analysis to ex-

amine the morphology and structure of NiO NPs. Fig. 5 (a-c) confirms the formation of agglomerated quasi-spherical particles. In Fig. 5d, sharp diffraction spots in the SAED pattern indicate a polycrystalline nature, consistent with XRD results.

Behera et al. demonstrate the synthesis of NiO NPs, confirmed through XRD. The XRD pattern in Fig. 6(a) shows no additional impurity peaks, indicating the crystalline nature of the NiO NPs. The intense diffraction peaks observed at  $37^\circ$ ,  $43^\circ$ ,  $63^\circ$ ,  $75^\circ$ , and  $79^\circ$  correspond to crystal planes (111), (200), (220), (311), and (222), respectively, consistent with the diffraction patterns of NiO NPs. Additionally, Scherrer's equation was used to determine that the average crystallite size of the NiO NPs was 22.8 nm. The FE-SEM image in Fig. 6(b) illustrates the surface morphology of the NiO. Most of the particles appear spherical, with some exhibiting a rod-like shape. The particle size ranges from 40 to 100 nm. Fig. 6(c) presents the EDX spectrum, confirming the elemental composition of the NiO nanoparticles. Lastly, the TEM image in Fig. 6(d) depicts spherical and rod-shaped NiO nanoparticles with diameters ranging from 10 to 80 nm [109].

As the green synthesis methods are now well-liked and popular among scientists, a considerable amount of literature has been published on the synthesis of NiO NPs by the use of different plants, and their details are given in Table 1.

## 2.2 Antibacterial applications of NiO NPs

Metallic oxide nanoparticles can be a suitable antibacterial tool. Biological features of metallic oxides NPs are related to their nano-based size and the high possibility of the NPs to interact with bio-objects [130, 131]. Over the last few years, more researchers have studied the antibacterial impacts of different metallic oxides on varied bacterial strains. As there have been more researches that focused on antibacterial applications of NiO NPs, we have considered reported antibacterial applications of NiO NPs on different bacterial strains such as *Streptococcus pneumoniae*, *Staphylococcus aureus*, *E. coli*, *E. hermannii* [132], *P. aeruginosa* [133], *B. anthracis*, *B. subtilis*, *Klebsiella pneumoniae*, *Enterobacter*

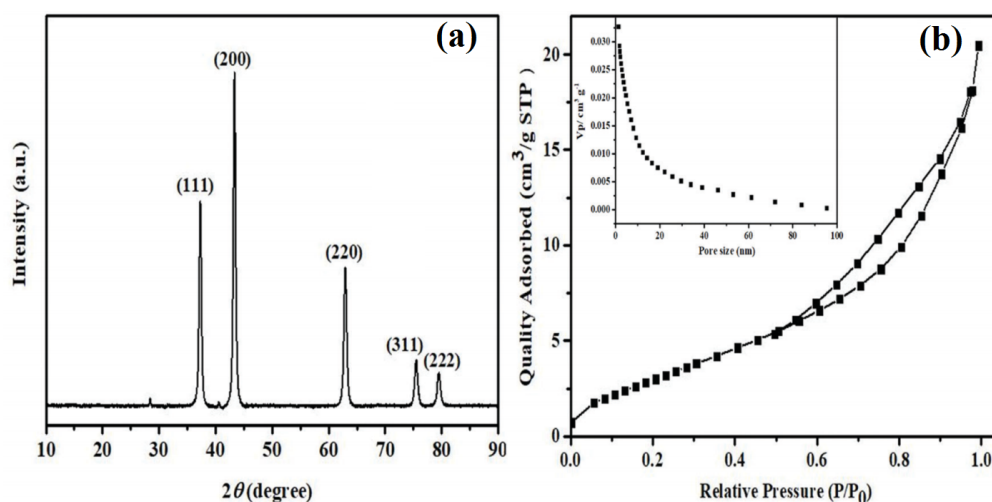


Figure 4. (a) XRD pattern, (b) BET (inset: pore size distribution) of the NiO NPs [105].

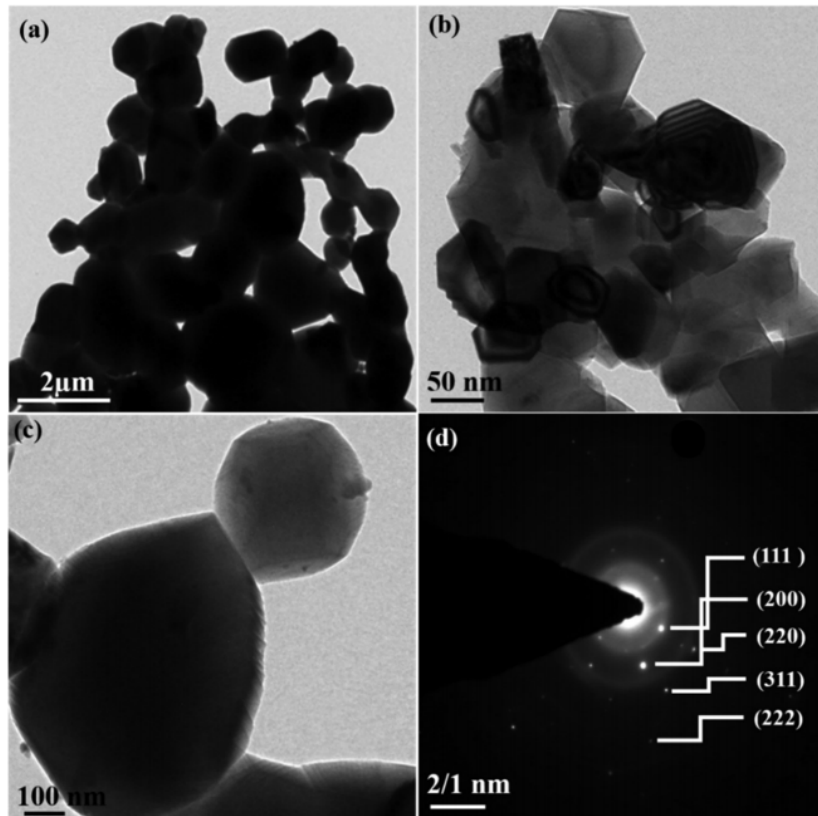


Figure 5. HRTEM images (a–c) and (d) SAED pattern of NiO NPs [105].

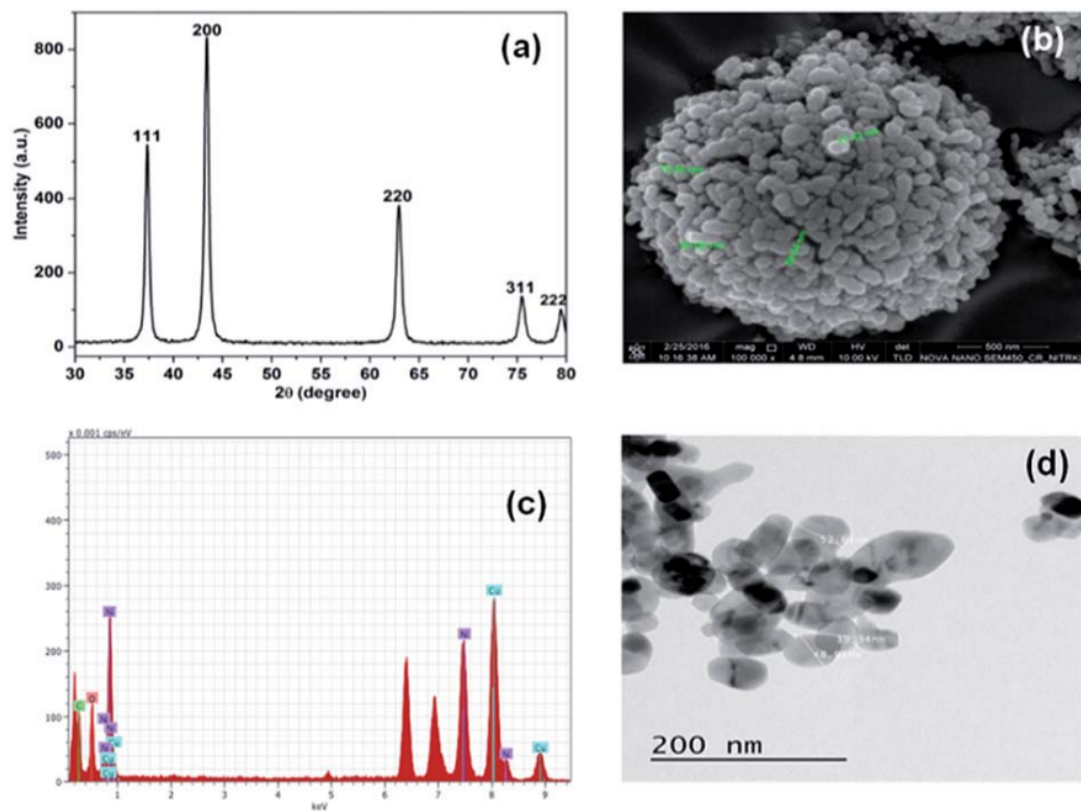


Figure 6. (a) XRD Pattern, (b) FESEM Image, (c) EDX and (d) TEM Image of NiO NPs [109].

**Table 1.** Plant mediated synthesis of NiO NPs.

| No. | Plant(family)                  | Part taken for extraction | Size (nm) | Shape                               | Ref.  |
|-----|--------------------------------|---------------------------|-----------|-------------------------------------|-------|
| 1   | Mytaceae                       | Red flower                | 20–35     | Quasi reversible with films         | [101] |
| 2   | Rutaceae                       | Leaf                      | 8–10      | Spherical                           | [91]  |
| 3   | Acacia tree                    | Sap                       | 34        | Cubic-spherical                     | [110] |
| 4   | Fabaceae                       | Flower                    | 6–10      | Crystalline                         | [92]  |
| 5   | Apocynaceae                    | Leaf                      | 20–40     | Spherical                           | [93]  |
| 6   | Moringaceae                    | Leaf                      | 5–10      | Spherical and slightly agglomerated | [111] |
| 7   | Lythraceae                     | Peel                      | 3         | Spherical and face-centered cubic   | [112] |
| 8   | Geraniceae                     | Leaf                      | 20–25     | Crystalline and spherical           | [106] |
| 9   | Rhamnaceae                     | Leaf                      | 18        | Spherical                           | [107] |
| 10  | Hydrangeaceae                  | Flower                    | 33        | Cubic crystalline                   | [108] |
| 11  | Tamaricaceae                   | Flower                    | 10–14     | Crystalline                         | [113] |
| 12  | Euphorbiaceae                  | Cassav waste              | 5–10      | Hexagonal and sphere                | [114] |
| 13  | Mytraceae                      | Leaf                      | 10–20     | Cubic                               | [115] |
| 14  | Apocynaceae                    | Leaf                      | 20        | Crystalline                         | [116] |
| 15  | Fabaceae                       | Root                      | 10–15     | Face-centered cubical structure     | [117] |
| 16  | Rutaceae                       | Leaf                      | 15–23     | Cubic crystalline                   | [118] |
| 17  | Sapindaceae                    | Rambutan peel waste       | 50–100    | Crystalline                         | [119] |
| 18  | Mytraceae                      | Leaf                      | 44        | Cubic and crystalline               | [100] |
| 19  | <i>Limonia acidissima</i>      | Fruit                     | 23        | Spherical                           | [120] |
| 20  | <i>Plectranthus amboinicus</i> | Leaf                      | 100       | Spherical                           | [121] |
| 21  | <i>Jatropha gossypifolia</i>   | Leaf                      | 30–40     | Rod shape                           | [122] |
| 22  | <i>Ageratum conyzoides</i>     | Leaf                      | 40–60     | Nanoflakes                          | [122] |
| 23  | <i>Senna auriculata</i>        | Flower                    | 20        | Spherical                           | [123] |
| 24  | <i>Nigella sativa</i>          | Seed                      | 10–50     | Spherical and oval                  | [124] |
| 24  | Olive                          | Leaf                      | 30–65     | Spherical                           | [125] |
| 25  | <i>Lantana camara</i>          | Flower                    | 40–50     | Oval                                | [126] |
| 26  | Orange                         | Leaf                      | 26–64     | Spherical and like oval             | [127] |
| 27  | Piper betle                    | Leaf                      | 20–40     | Spherical                           | [128] |
| 28  | Aloe vera                      | Leaf                      | –         | –                                   | [129] |

*aerogenes* [134], *S. pyogenes*, and *Proteus vulgaris* [135]. The other synthesized NiO NPs with different antibacterial capabilities are listed in Table 2.

### 2.3 Photocatalytic applications of NiO NPs

Organic pollutants, which are released from industrial sectors, might be the biggest threat to our environment as they are highly poisonous and harmful to a variable microorganism [148–151]. The hazardous pollutants degradation has gained more attention, so photocatalytic degradations in the presence of different light sources is said to be an applicable factor for organic pollutant degradation [60, 152–158]. Nano-based semiconductors like CuO, ZnO, TiO<sub>2</sub>, etc. have been the most sufficient photocatalysts for organic pollutants degradation [159–165].

Ahmad Khan and colleagues elucidate semiconductor photocatalysis, wherein photons with energy equal to or greater

than the bandgap energy of the photocatalyst are required. Upon light irradiation on the nanoparticles (NPs), electrons (e<sup>-</sup>) in the valence band (VB) are excited to the conduction band (CB), creating positively charged holes (h<sup>+</sup>) in the VB. The conduction band electrons (e<sup>-</sup>) react with O<sub>2</sub> species as electron acceptors, forming the strong oxidizing agent superoxide anion radical (·O<sub>2</sub><sup>-</sup>). Similarly, h<sup>+</sup> in the VB reacts with H<sub>2</sub>O molecules, generating hydroxyl radicals (·OH). Both radicals are responsible for dye degradation [166]. The degradation mechanism is illustrated in Fig 7. Among different nanoparticles which are used as photocatalysts, NiO NPs have been utilized for the degradation of various dyes, such as Methylene blue [136], Methyl orange [167], Evans blue [168], Rhodamine B [169], Rose Bengal [134], Reactive black [170], Congo Red [171], Violet dye [172], Acid scarlet dye [173], and Trypan Blue [144], as well as different organic pollutant degradations

**Table 2.** Antibacterial applications of NiO nanoparticles.

| Synthetic approach                                         | Bacterial strain                           | Zone of Inhibition | Morphology                                  | Crystallite Size (based on XRD) | Reference |
|------------------------------------------------------------|--------------------------------------------|--------------------|---------------------------------------------|---------------------------------|-----------|
| Hot plate combustion method                                | <i>S. pneumoniae</i>                       | 12 mm              | Cubic and spherical shape                   | 8–10 nm                         | [132]     |
|                                                            | <i>S. aureus</i>                           | 16 mm              |                                             |                                 |           |
|                                                            | <i>E. coli</i>                             | 11 mm              |                                             |                                 |           |
|                                                            | <i>E. hermannii</i>                        | 6 mm               |                                             |                                 |           |
| Hydrothermal                                               | <i>S. aureus</i><br><i>E. coli</i>         | –                  | Disk like                                   | NiO-300 = 5nm                   | [136]     |
|                                                            |                                            |                    |                                             | NiO-400 = 6.8 nm                |           |
|                                                            |                                            |                    |                                             | NiO-500 = 12.7 nm               |           |
| Thermal decomposition                                      | <i>E. coli</i>                             | 12 mm              | Rod like                                    | 60 nm                           | [133]     |
|                                                            | <i>P. aeruginosa</i>                       | 11 mm              |                                             |                                 |           |
|                                                            | <i>S. aureus</i>                           | 10 mm              |                                             |                                 |           |
| Hot combustion reaction                                    | <i>S. pneumoniae</i>                       | 22.4 mm            | Stick like                                  | 50 nm                           | [134]     |
|                                                            | <i>B. anthracis</i>                        | 25.4 mm            |                                             |                                 |           |
|                                                            | <i>K. pneumoniae</i>                       | 23.2 mm            |                                             |                                 |           |
|                                                            | <i>E. aerogenes</i>                        | 27.5 mm            |                                             |                                 |           |
|                                                            | <i>B. subtilus</i>                         | –                  |                                             |                                 |           |
| Biosynthetic method                                        | <i>S. aureus</i>                           | NiO: 10 mm         | Hexagonal crystal phase<br>And oblong shape | 12 nm                           | [137]     |
|                                                            |                                            | NiO-350: 11 mm     |                                             |                                 |           |
|                                                            |                                            | NiO-450:15 mm      |                                             |                                 |           |
|                                                            | <i>E. coli</i>                             | NiO: 11 mm         |                                             |                                 |           |
|                                                            |                                            | NiO-350: 13 mm     |                                             |                                 |           |
|                                                            |                                            | NiO-450: 15 mm     |                                             |                                 |           |
| Pulsed laser ablation                                      | <i>S. aureus</i>                           | 12.6 ± 0.57 mm     | Spherical                                   | 2–21 nm                         | [138]     |
|                                                            | <i>E. coli</i>                             | 14.3 ± 1.15 mm     |                                             |                                 |           |
| Green method using <i>Eucalyptus globulus</i> leaf extract | <i>E. coli</i> -60                         | 17 mm              | –                                           | 10–20 nm                        | [115]     |
|                                                            | <i>E. coli</i> -52                         | 17 mm              |                                             |                                 |           |
|                                                            | <i>P. aeruginosa</i> -48                   | 15 mm              |                                             |                                 |           |
|                                                            | <i>P. aeruginosa</i> -64                   | 14 mm              |                                             |                                 |           |
|                                                            | Methicillin sensitive <i>S. aureus</i> -06 | 15 mm              |                                             |                                 |           |
|                                                            | Methicillin sensitive <i>S. aureus</i> -02 | 13 mm              |                                             |                                 |           |
|                                                            | Methicillin resistant <i>S. aureus</i> -10 | 15 mm              |                                             |                                 |           |
|                                                            | Methicillin resistant <i>S. aureus</i> -31 | 14 mm              |                                             |                                 |           |
| Sol-gel                                                    | <i>E. coli</i>                             | 10 mm              | Cubic and irregular shape                   | 30 nm                           | [139]     |
|                                                            | <i>K. pneumoniae</i>                       | 0                  |                                             |                                 |           |
|                                                            | <i>P. vulgaris</i>                         | 0                  |                                             |                                 |           |
|                                                            | <i>S. mutans</i>                           | 8 mm               |                                             |                                 |           |
|                                                            | <i>B. subtilus</i>                         | 12 mm              |                                             |                                 |           |
|                                                            | <i>S. aureus</i>                           | 11 mm              |                                             |                                 |           |

Continued on next page

**Table 2.** Antibacterial applications of NiO nanoparticles. (Continued)

| Synthetic approach                                       | Bacterial strain          | Zone of Inhibition                 | Morphology                            | Crystallite Size (based on XRD) | Reference |
|----------------------------------------------------------|---------------------------|------------------------------------|---------------------------------------|---------------------------------|-----------|
| Co-precipitation                                         | E. coli                   | Maximum zone of inhibition = 15 mm | Cubic and spherical shape             | 30 nm                           | [140]     |
|                                                          | K. pneumoniae             |                                    |                                       |                                 |           |
|                                                          | B. subtilus               |                                    |                                       |                                 |           |
|                                                          | S. aureus                 |                                    |                                       |                                 |           |
| Green synthetic routes using <i>Calotropis gigantea</i>  | E. coli                   | –                                  | –                                     | < 60 nm                         | [93]      |
|                                                          | B. subtilus               | –                                  |                                       |                                 |           |
| Green method using <i>Monsonia burkenea</i> leaf extract | E. coli                   | –                                  | Spherical shape                       | 25 nm                           | [106]     |
|                                                          | P. aeruginosa             |                                    |                                       |                                 |           |
|                                                          | Enterococcus faecalis     |                                    |                                       |                                 |           |
|                                                          | S. aureus                 |                                    |                                       |                                 |           |
| Microwave-assisted route                                 | P. aeruginosa             | 13.67 ± 0.29 mm                    | Spherical shape                       | 20 nm                           | [141]     |
|                                                          | E. coli                   | 15.37 ± 0.17 mm                    |                                       |                                 |           |
|                                                          | K. pneumoniae             | 13.80 ± 0.29 mm                    |                                       |                                 |           |
|                                                          | S. aureus                 | 14.67 ± 0.17 mm                    |                                       |                                 |           |
| Co-precipitation method                                  | E. coli (5 mg/ml) RT      | 14 mm                              | –                                     | –                               | [142]     |
|                                                          | E. coli (3 mg/ml) RT      | 12 mm                              |                                       |                                 |           |
|                                                          | E. coli (5 mg/ml) RT 60   | 16mm                               |                                       |                                 |           |
|                                                          | E. coli (3 mg/ml) RT 60   | 15 mm                              |                                       |                                 |           |
|                                                          | S. aureus (5 mg/ml) RT    | 11 mm                              |                                       |                                 |           |
|                                                          | S. aureus (5 mg/ml) RT    | 7mm                                |                                       |                                 |           |
|                                                          | S. aureus (5 mg/ml) RT 60 | 15 mm                              |                                       |                                 |           |
|                                                          | S. aureus (3 mg/ml) RT 60 | 18 mm                              |                                       |                                 |           |
| Sol-gel                                                  | E. coli                   | –                                  | Grainy                                | 30–80 nm                        | [143]     |
|                                                          | S. aureus                 |                                    |                                       |                                 |           |
| Co-precipitation                                         | S. aureus                 | 9.8 mm                             | Spherical and cubical shape           | 40 nm                           | [135]     |
|                                                          | S. pyogenes               | 9.0 mm                             |                                       |                                 |           |
|                                                          | B. subtilus               | 8.5 mm                             |                                       |                                 |           |
|                                                          | P. aeruginosa             | 8.3 mm                             |                                       |                                 |           |
|                                                          | K. pneumoniae             | 8.1 mm                             |                                       |                                 |           |
| Combustion method                                        | K. aerogenes              | –                                  | Bunsenite form of simple cubic system | 28 nm                           | [144]     |
|                                                          | E. coli                   | –                                  |                                       |                                 |           |
|                                                          | P. aeruginosa             | 4.12 ± 0.43                        |                                       |                                 |           |
|                                                          | S. aureus                 | –                                  |                                       |                                 |           |
| Microwave-Assisted                                       | S. aureus                 | 24 ± 0.9                           | Spherical                             | 15–16 nm                        | [135]     |
|                                                          | P. vulgaris               | 19 ± 0.9                           |                                       |                                 |           |
|                                                          | E. coli                   | 25 ± 0.3                           |                                       |                                 |           |
|                                                          | P. aeruginosa             | 24 ± 0.6                           |                                       |                                 |           |

Continued on next page



**Table 2.** Antibacterial applications of NiO nanoparticles. (Continued)

| Synthetic approach                                | Bacterial strain     | Zone of Inhibition | Morphology              | Crystallite Size (based on XRD) | Reference |
|---------------------------------------------------|----------------------|--------------------|-------------------------|---------------------------------|-----------|
| Green method using <i>Rhamnus virgata</i> extract | <i>S. aureus</i>     | 20 mm              | Spherical               | 24 nm                           | [145]     |
|                                                   | <i>B. subtilis</i>   | 29 mm              |                         |                                 |           |
|                                                   | <i>P. aeruginosa</i> | 16 mm              |                         |                                 |           |
|                                                   | <i>K. pneumoniae</i> | 14 mm              |                         |                                 |           |
|                                                   | <i>E. coli</i>       | 27 mm              |                         |                                 |           |
| Co-precipitation                                  | <i>E. coli</i>       | –                  | Spherical and cubic     | 12–16 nm                        | [146]     |
|                                                   | <i>S. aureus</i>     | –                  |                         |                                 |           |
| Electrospray method                               | <i>E. coli</i>       | –                  | –                       | 20 nm                           | [147]     |
| Biogenic synthesis                                | <i>Proteus</i>       | 1.1 cm             | Spherical               | –                               | [121]     |
| Green method using <i>Jatropha gossypifolia</i>   | <i>B. subtilis</i>   | 4.1 mm             | Rod                     | 30–40 nm                        | [122]     |
|                                                   | <i>B. cereus</i>     | 3.6 mm             |                         |                                 |           |
|                                                   | <i>S. aureus</i>     | 6.2 mm             |                         |                                 |           |
|                                                   | <i>Klebsiella</i>    | 3.5 mm             |                         |                                 |           |
| Green synthesis                                   | <i>B. subtilis</i>   | 21 mm              | Spherical               | 3.92 nm                         | [123]     |
|                                                   | <i>S. aureus</i>     | 20 mm              |                         |                                 |           |
|                                                   | <i>P. aeruginosa</i> | 21 mm              |                         |                                 |           |
|                                                   | <i>E. coli</i>       | 23 mm              |                         |                                 |           |
| Solution combustion                               | <i>E. coli</i>       | Nio-1: –           | Oval                    | Nio-1: 14.3 nm                  | [126]     |
|                                                   |                      | Nio-2: –           |                         |                                 |           |
|                                                   |                      | Nio-3: 12.33 mm    |                         |                                 |           |
|                                                   | <i>M. luteus</i>     | Nio-1: 10.67 mm    |                         | Nio-2: 20 nm                    |           |
|                                                   |                      | Nio-2: 11.67 mm    |                         |                                 |           |
|                                                   |                      | Nio-3: 10.33 mm    |                         |                                 |           |
|                                                   | <i>S. aureus</i>     | Nio-1: 11.67 mm    |                         | Nio-3: 26 nm                    |           |
|                                                   |                      | Nio-2: 15 mm       |                         |                                 |           |
|                                                   |                      | Nio-3: 13.33 mm    |                         |                                 |           |
| Green synthesis                                   | <i>E. coli</i>       | 25 mm              | Spherical and like oval | 20.34–27.04 nm                  | [127]     |
|                                                   | <i>S. aureus</i>     | 32 mm              |                         |                                 |           |
| Green synthesis                                   | <i>E. coli</i>       | 20 mm              | Spherical               | 26.27 nm                        | [128]     |
|                                                   | <i>B. subtilis</i>   | 25 mm              |                         |                                 |           |
| Green synthesis                                   | <i>E. coli</i>       | 18 mm              | –                       | 22 nm                           | [129]     |
|                                                   | <i>P. multocida</i>  | 19 mm              |                         |                                 |           |
|                                                   | <i>B. subtilis</i>   | 23 mm              |                         |                                 |           |
|                                                   | <i>S. aureus</i>     | 25 mm              |                         |                                 |           |

like NO destruction [174], 4-chlorophenol [132], Phenol [175], Acetaldehyde [176], Acid fuchsine [177], Whole of the reported photocatalytic applications of NiO NPs in organic pollutants degradation listed in Table 3.

#### 2.4 Catalytic applications of NiO NPs

Biodegradable, green, and costless metallic oxides NPs, such as ZnO, CuO, NiO, MgO, and CdO, have been com-

prehensively surfed as selective catalysts in C-C and C-heteroatom reactions [179]. These nanoparticles and their performance in multicomponent reactions (MCRs) have gained considerable attention in the last decade [180–187]. A Proficient and suitable property of MCRs over the conventional synthetic approaches is that the MCRs are one spot, cheaper as well as being energy and time-sufficient [188, 189]. Some articles have presented the procedure

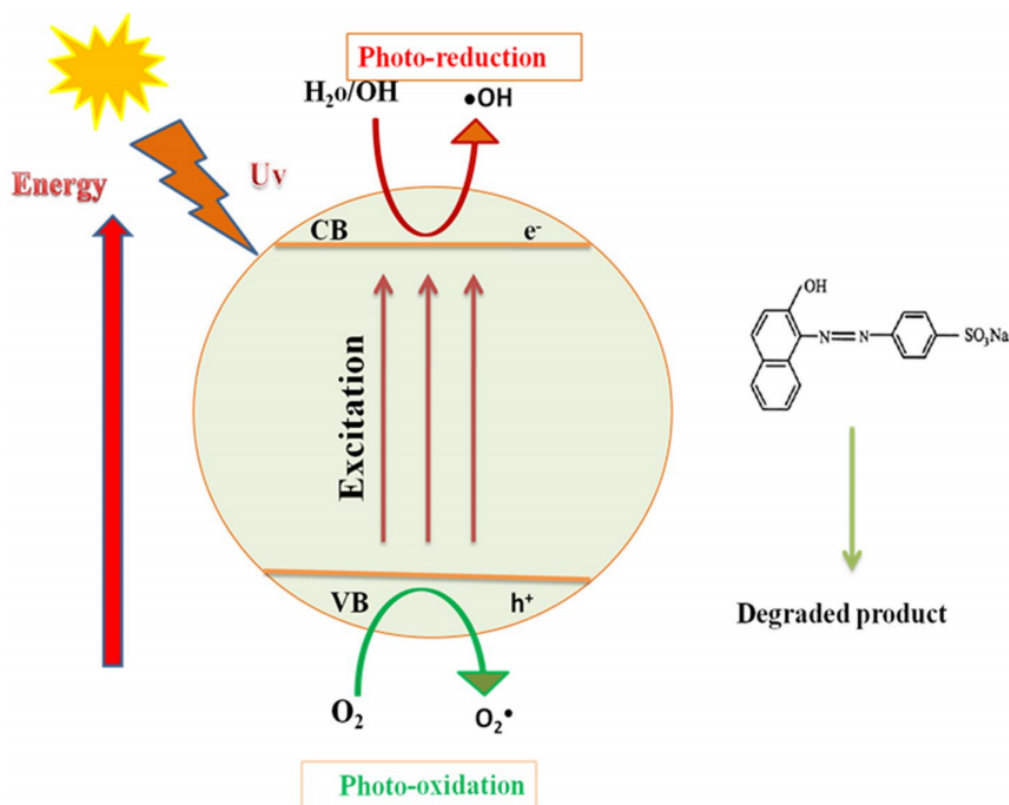
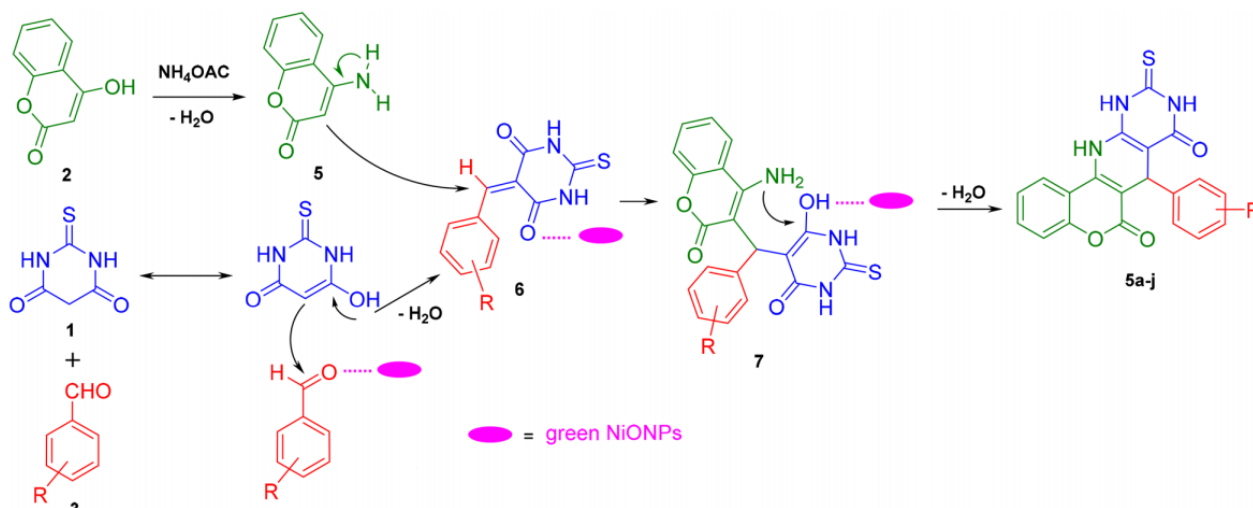


Figure 7. Illustrative mechanism of photocatalytic degradation using NiO NPs [166].

of various reported metallic oxides nanoparticles catalyzed by different MCRs for vital organic compounds synthesis. Herein, among the mentioned metallic oxide NPs, NiO NPs catalytic applications in MCRs have been considered. Scheme 1 demonstrates a catalyzed sequential multicomponent reaction route proposed by Moavi and colleagues. The enol form of thiobarbituric acid (1) undergoes Knoevenagel condensation with the catalyst-activated carbonyl of an aryl aldehyde (3) to give the  $\alpha,\beta$ -unsaturated molecule 6, followed by dehydration. Subsequently, 4-hydroxycoumarin (2) reacts at 100 °C with in situ generated ammonia

from ammonium acetate (4) to form 4-aminocoumarin (5). Michael's addition of the enamine (5) to the  $\alpha,\beta$ -unsaturated carbonyl acceptor of 6 yields the intermediate 7. After the elimination of H<sub>2</sub>O, an amino group attacks the carbonyl group with NiO catalyst to cyclize the intramolecular ring to give the desired products 5 in an aqueous medium. The addition of algal NiO NPs to the process enhances the electrophilicity and facilitates the attack of nucleophilic groups due to their acidity. In addition, the Lewis acid NiO nanocatalyst improves the reactivity of the organic material and the stability of the intermediates [178].



Scheme 1. Proposed mechanism for pyridopyrimidine derivatives synthesis using the NiO NPs [178].

Table 3. Photocatalytic efficiency of NiO nanoparticles in the degradation of organic pollutants.

| Synthetic approach                                                                       | Pollutant type | Pollutant concentration | Morphology                                                                                           | Time                                      | Light source               | Catalyst concentration | Crystallite Size based on XRD  | Degradation efficiency                                     | Ref.  |
|------------------------------------------------------------------------------------------|----------------|-------------------------|------------------------------------------------------------------------------------------------------|-------------------------------------------|----------------------------|------------------------|--------------------------------|------------------------------------------------------------|-------|
| Thermal decomposition                                                                    | NO destruction | 1 mg/L                  | Hexagonal Quasi-hexagonal                                                                            | 30 min                                    | High pressure Mercury lamp | –                      | 400 nm                         | 21%                                                        | [174] |
| hot plate combustion method using Aegle marmelos plant                                   | 4-Chlorophenol | 50–250 mg/L<br>100 mg/L | pure face centered cubic phase and single crystalline, spherical                                     | 30 min                                    | Low pressure Mercury lamp  | 30 mg                  | 8–10 nm                        | 87% over 120 min                                           | [132] |
| Hydrothermal                                                                             | Methylene blue | 15 mg/L                 | Disk shaped and spherical                                                                            | 20 min                                    | UV-Visible                 | 1 mg                   | 5.1 nm                         | 98.7% (Blue dye)<br>94–97.6% (other mixture)               | [136] |
| Thermal decomposition                                                                    | Methylene blue | 10 mg/L                 | Crystalline                                                                                          | 30 min for NiO-400 and 90 min for NiO-300 | UV-Visible<br>Green light  | 5 mg                   | 14 nm<br>6–10 nm at 300–400 °C | 46% for NiO-300 and NiO-400 was 3 times as that of NiO-300 | [92]  |
| Thermal-decomposition (A), sol-gel (B), hydrothermal (C), and emulsion (D) nano-reactors | Methyl orange  | 40 mg/L                 | Spherical<br>A: flower like shape<br>B: shape of regular nano-woods<br>C: plate-like<br>D: spherical | 120 min                                   | UV-Visible<br>Green light  | 20 mg                  | 100 nm                         | 86%                                                        | [167] |
| Sol-gel method                                                                           | Phenol         | 100 mg/L                | Spherical                                                                                            | 60 min                                    | UV laser                   | 100 mg                 | 6–10 nm                        | 97%                                                        | [175] |
| Chemical precipitation method                                                            | Methylene Blue | $1 \times 10^{-5}$ M    | Oval shape                                                                                           | 150 min                                   | Solar light                | 0.031 g                | 64 nm                          | –                                                          | [190] |
| Combustion method                                                                        | Methyl orange  | 0.1 mM                  | Octahedral shape                                                                                     | –                                         | UV                         | 0.0125 mM              | 50 nm                          | –                                                          | [191] |
| Microwave-assisted method                                                                | Evans blue     | –                       | Spherical                                                                                            | 120 min                                   | Solar light                | 20 mg                  | 24 nm                          | 88%                                                        | [168] |
| Thermal decomposition                                                                    | Methylene Blue | 5 mg                    | Coral-like                                                                                           | 90 min                                    | Solar light                | 1 mg                   | 2–3 nm                         | $\geq 97\%$                                                | [192] |
| Thermal decomposition                                                                    | Rhodamine B    | –                       | Sheet-like                                                                                           | 120 min                                   | Osram ultraviolet lamp     | –                      | 10 nm                          | 80%                                                        | [169] |

Continued on next page

Table 3. Photocatalytic efficiency of NiO nanoparticles in the degradation of organic pollutants. (Continued)

| Synthetic approach                                      | Pollutant type                  | Pollutant concentration | Morphology                        | Time       | Light source                              | Catalyst concentration | Crystallite Size based on XRD | Degradation efficiency  | Ref.  |
|---------------------------------------------------------|---------------------------------|-------------------------|-----------------------------------|------------|-------------------------------------------|------------------------|-------------------------------|-------------------------|-------|
| Thermal decomposition                                   | Methylene Blue                  | 25 mg/L                 | Rod-like                          | 135 min    | 250 W highpressure mercury lamp (GYZ-250) | 15 mg/L                | 20 nm                         | 99%                     | [193] |
| Co-precipitation                                        | Acetaldehyde                    | 8 M                     | Rime-like                         | 120 min    | UV                                        | 6.5 ± 0.1 mg           | –                             | 98%                     | [176] |
| Solvothermal                                            | Methylene Blue                  | 20 mg/L                 | Rocksalt cubic face               | 140 min    | 300 W Xe arc Lamp                         | 0.1 g                  | 5–10 nm                       | 100%                    | [194] |
| Hot combustion reaction                                 | Rose Bengal                     | 10 mg/L                 | Stick like                        | 100 min    | UV                                        | 50 mg                  | 50 nm                         | –                       | [134] |
| Calcination method                                      | Phenol                          | 0.02 mg/L               | Spherical NiO Hexagonal NiO       | 100 min    | UV                                        | 0.22 mg                | 5–10 nm 22–27 nm              | 82% ≥ 69%               | [195] |
| Thermal decomposition                                   | Reactive black 5 Methylene Blue | 3 × 10 <sup>-5</sup> M  | Simple cubic structure            | 60 min 5 h | Tungsten halogen lamps                    | 30 mg                  | –                             | RB-5 = 87.2% MB = 70.2% | [170] |
| solid-state thermal decomposition                       | Methylene Blue (MB)             | 5 mg/L                  | Spherical                         | 120 min    | UV                                        | 20 mg                  | 20–50 nm                      | 98%                     | [196] |
| Co-precipitation                                        | Methylene Blue                  | –                       | Face cubic                        | 270 min    | UV                                        | –                      | 10–28 nm                      | 89%                     | [197] |
| Solvothermal                                            | Acid fuchsin                    | 20.0 mg/L               | Rose-like                         | 30 min     | 300 W medium-pressure mercury lamp        | 1.0 g L <sup>-1</sup>  | 3–4 nm                        | 100%                    | [177] |
| Hydrothermal                                            | Congo Red                       | 10 mg/L                 | Cube shape                        | 30 min     | Mercury lamp                              | 0.1 g                  | 20 nm                         | 98%                     | [171] |
| Precipitation                                           | Violet dye                      | –                       | Sphere like                       | 50 min     | UV                                        | 50 mg                  | 20 nm                         | 98%                     | [172] |
| Hydrothermal                                            | Methylene Blue                  | 10 mg/L                 | Face centered cubic               | 60 min     | UV                                        | 1.0 g                  | ≤ 100 nm                      | ≤ 47%                   | [198] |
| Thermal decomposition                                   | DFB                             | 75 mg/L                 | Spherical and face-centered cubic | 150 min    | Mercury lamp                              | 10 mg                  | 50 nm                         | 96.4%                   | [199] |
| Pulsed laser deposition                                 | Rhodamine B                     | 10 mg/L                 | Thin films                        | 60 min     | Xe lamp                                   | –                      | 8–16 nm                       | –                       | [200] |
| Thermal decomposition                                   | Acid scarlet                    | 20 mg/L                 | Wire like                         | 60 min     | 15 W ultraviolet (UV) lamps               | 10 mg                  | 8–12 nm                       | –                       | [173] |
| Green synthetic routes using <i>Calotropis gigantea</i> | Methylene Blue                  | 0.08 mM                 | –                                 | –          | Sun light                                 | 0.01 g                 | < 60 nm                       | 98.6%                   | [93]  |

Continued on next page

**Table 3.** Photocatalytic efficiency of NiO nanoparticles in the degradation of organic pollutants. (Continued)

| Synthetic approach                                       | Pollutant type   | Pollutant concentration | Morphology                            | Time    | Light source  | Catalyst concentration | Crystallite Size based on XRD | Degradation efficiency | Ref.  |
|----------------------------------------------------------|------------------|-------------------------|---------------------------------------|---------|---------------|------------------------|-------------------------------|------------------------|-------|
| Co-precipitation                                         | Congo red dye    | 20 mg/L                 | Cubic and spherical shape             | 30 min  | UV            | 5 mg                   | 30 nm                         | 84%                    | [140] |
| Green method using <i>Monsonia burkenae</i> leaf extract | Methylene Blue   | 20 mg/L                 | Spherical shape                       | 75 min  | 15 W LED      | 20 mg                  | 25 nm                         | 50%                    | [106] |
| Microwave-assisted method                                | Evans blue       | –                       | Spherical shape                       | 150 min | Sunlight      | 20 mg                  | 20 nm                         | 91%                    | [141] |
| Combustion method                                        | Trypan Blue      | 100 mg/L                | Bunsenite form of simple cubic system | 150 min | UV            | 10 mg                  | 40 nm                         | 98%                    | [144] |
| Green combustion                                         | Methylene Blue   | 1 mM                    | Spherical                             | 90 min  | UV            | 40 mg                  | 23 nm                         | 99.6%                  | [120] |
| Green synthesis                                          | Methylene Blue   | 10 g/L                  | Spherical                             | 90 min  | sunlight      | 0.2 g/L                | 3.92 nm                       | 97%                    | [123] |
| solution combustion                                      | Methylene Blue   | 10 mg/L                 | oval                                  | 60 min  | UV            | 30 mg                  | 14.3–26 nm                    | 96–98%                 | [126] |
| Green synthesis                                          | Reactive Red 141 | 50 mg/L                 | Spherical                             | 100 min | Visible Light | 15 mg                  | 26.27 nm                      | 99%                    | [128] |
| Green synthesis                                          | methylene blue   | 50 mg/L                 | triangular                            | 13 min  | UV            | 10 mg                  | 7–20 nm                       | 98%                    | [201] |
| Green sonochemical                                       | Safranin         | 1 mg/L                  | Spherical                             | 100 min | UV            | 5 mg                   | 9.38 nm                       | 92.75%                 | [202] |
| Green sonochemical                                       | Methyl orange    | 1 mg/L                  | Spherical                             | 100 min | UV            | 5 mg                   | 9.38 nm                       | 98%                    | [202] |
| Biosynthesis                                             | Rhodamine-B      | 20 mg/L                 | Spherical                             | 90 min  | Visible Light | 20 mg                  | 12 nm                         | 85%                    | [203] |
| Precipitation                                            | Rhodamine B      | 0.025 mg/L              | Spherical                             | 16 min  | Solar light   | 0.5 mg                 | –                             | 98                     | [204] |
| Biosynthesis                                             | Methylene Blue   | 20 mg/L                 | flowerlike                            | 270 min | UV            | 20 mg                  | 18.4 nm                       | 86                     | [205] |
| Biosynthesis                                             | Malachite Green  | 20 mg/L                 | flowerlike                            | 210 min | UV            | 20 mg                  | 18.4 nm                       | 98                     | [205] |



### 2.4.1 Synthesis of pyrroles

Bhalchandra M. Bhanage et al. reported the synthesis of substituted pyrroles via amines, aldehydes, nitroalkanes, and 1,3-dicarbonyl compounds in one pot synthesis reaction which catalyzed by NiO NPs at ambient temperature. They figured out that NiO NPs could be a trustable catalyst, due to having suitable activity and features, for a broad range of different substrates with desirable yields of focused products along with catalyst reusability [206] (Scheme 2).

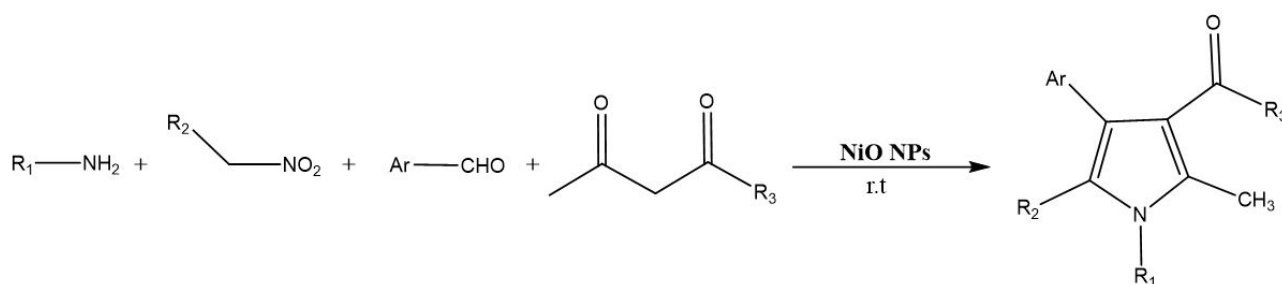
### 2.4.2 Synthesis of amidoalkyl naphthol derivatives

Ratiram G. et al. reported the synthesis of amidoalkyl naphthol derivatives by means of applicable and appropriate

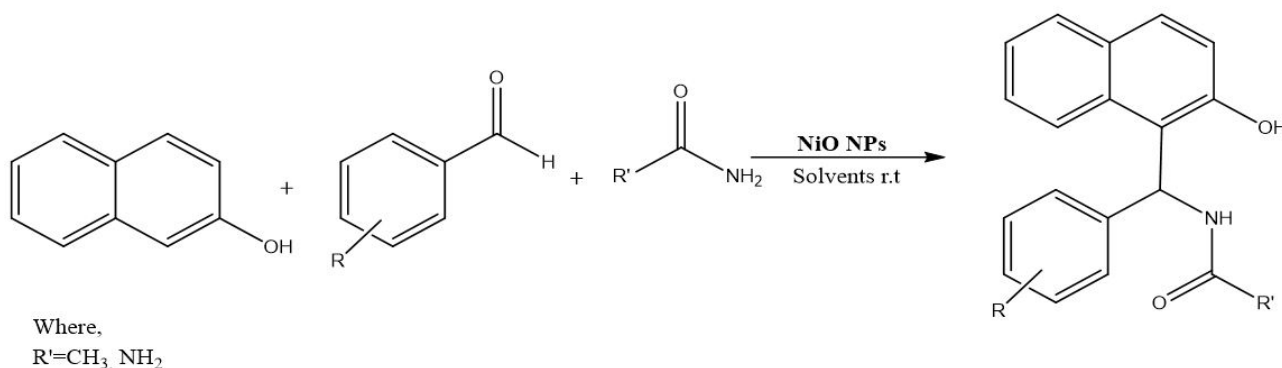
NiO NPs catalyst and using condensation reaction of urea,  $\beta$ -naphthol, and aldehydes. The advantages of this synthetic method were simple workup, solvent free usage, and highly reusability of its catalyst [207] (Scheme 3).

### 2.4.3 Synthesis of varied spiro and condensed indole derivatives

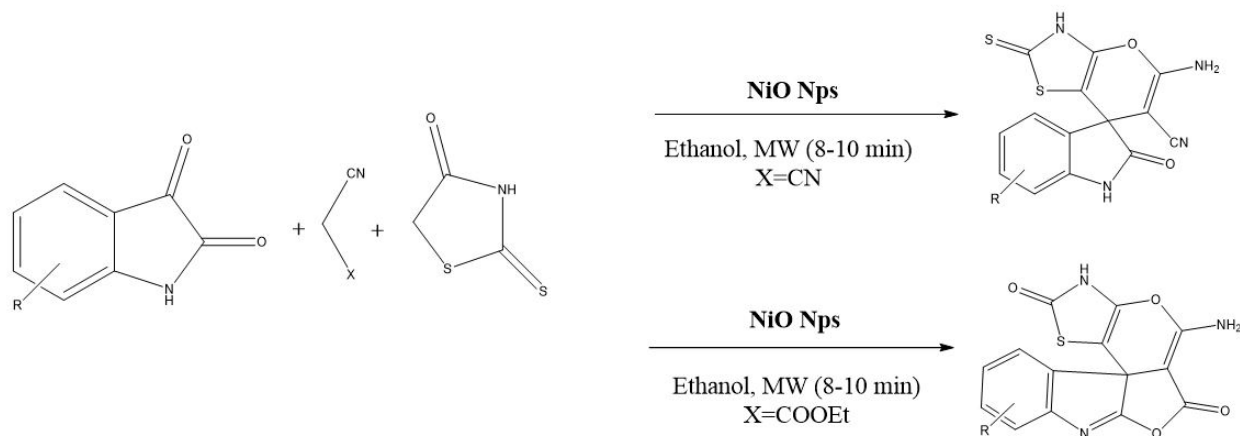
Another study investigated the synthesis of different spiro and condensed indole derivatives by means of substituted 1H-indole-2,3-diones, 2-thioxo-4-thiazolidinone, and methylene as a reagent as well as highly efficient NiO NPs as a catalyst. The reaction was engaged in Michael and Knoevenagel condensation (Scheme 4). Work simplicity,



Scheme 2. Synthesis of pyrroles by using NiO NPs.



Scheme 3. Synthesis of amidoalkyl naphthols derivatives by using NiO NPs.



Scheme 4. Synthesis of spiro and condensed indole derivatives.

easy-to-handle, and convincing yields make the catalytic approach more applicable [208].

#### 2.4.4 Synthesis of 2-substituted-4, 6- diarylpyrimidines

A trusted and economical-friendly approach has recently been proposed for the synthesis of 2-substituted-4, 6- diarylpyrimidines in the one-pot reaction between S-benzylthiouonium chloride, morpholine, and varied substituted chalcones by means of NiO NPs as a reproducible and costless catalyst. The reaction could improve the catalytic synthesis of 2-(4-morpholinyl)-4,6-diarylpyrimidines with a proper yield and short reaction time [209] (Scheme 5).

#### 2.4.5 Synthesis of 2-(1H-tetrazol-5-yl) acrylonitrile derivatives

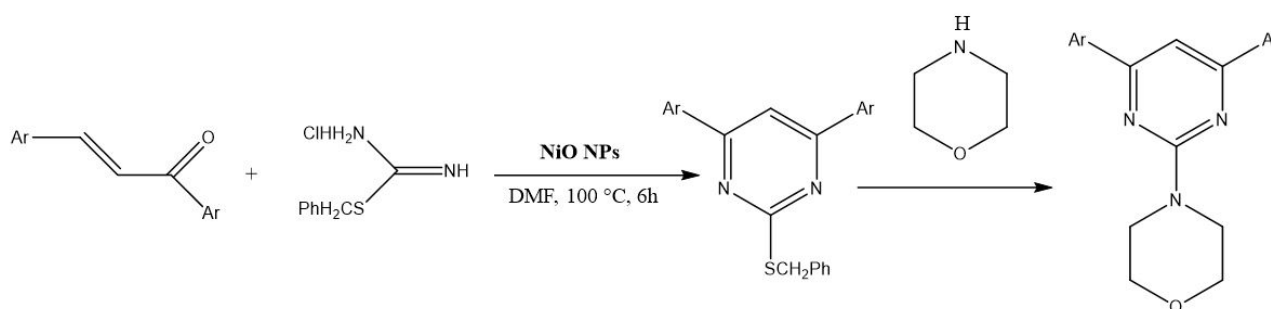
A novel and rapid procedure of 2-(1H-tetrazol-5-yl) acrylonitrile derivatives synthesis has recently been fulfilled using one pot MCRs of malononitrile, aldehydes, and sodium azide which required NiO nanoparticles as a reproducible catalyst (Scheme 6). Safaei-Ghomi et al. stated that this method has a suitable features such as easy to work, shorter

reaction time in comparison with traditional methods, and high yields as well as reusability of catalyst [210].

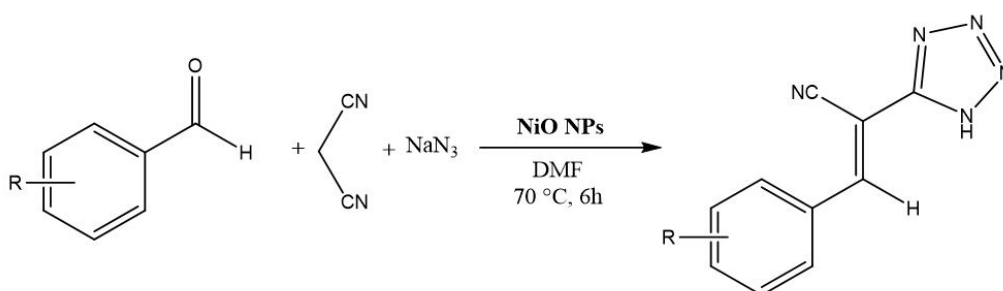
#### 2.4.6 Synthesis of 3,4-dihydropyrimidin-2(1H)-ones

Khashaei and coworkers discovered a method for producing 3,4-dihydropyrimidin-2(1H)-ones (DHPMs) using a NiO NPs catalyst. This involved a condensation reaction between urea, ethyl/methyl acetoacetate, and an arylaldehyde. The technology offers several benefits, including the production of pure NiO nanoparticles through a unique route and their utilization as a low-toxic, affordable, and efficient catalyst for DHPM synthesis [211] (Scheme 7).

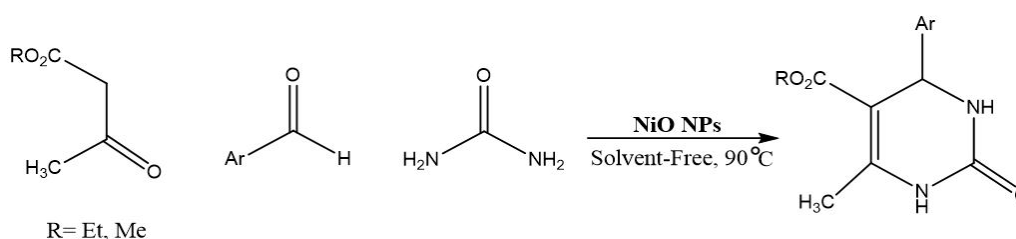
Scheme 8 illustrates the reaction catalyzed by NiO nanoparticles to produce the target product. The process initiates by activating arylaldehydes and  $\beta$ -ketoester, leading to the formation of enol-tautomeric forms. Subsequent Knoevenagel condensation results in the formation of intermediate  $\alpha,\beta$ -unsaturated ketones. Activated urea molecules undergo Michael-type addition, yielding an open-chain ureide intermediate, which cyclizes to form the target DHPMs, six-membered heterocyclic compounds. NiO accelerates



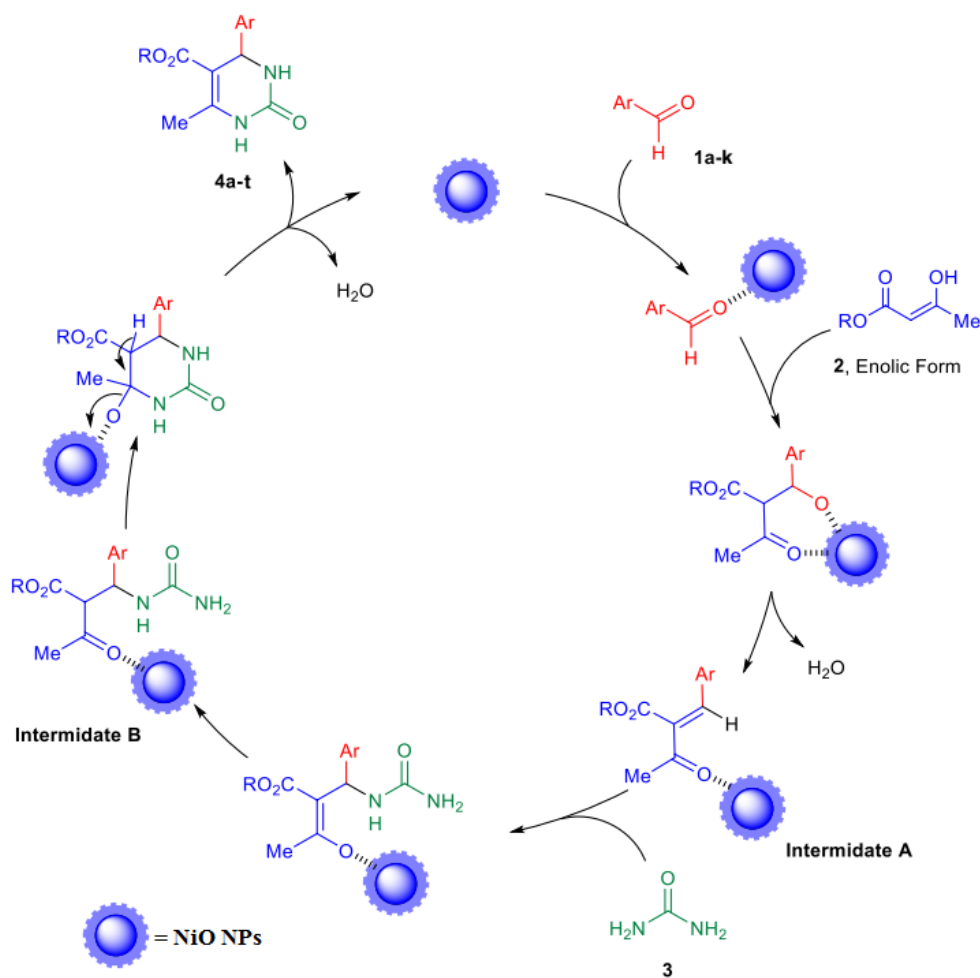
**Scheme 5.** Synthesis of 2-(4-morpholinyl)-4,6-diarylpyrimidines by means of NiO nanoparticles.



**Scheme 6.** Synthesis of 2-(1H-tetrazol-5-yl) acrylonitrile derivatives using NiO NPs.



**Scheme 7.** Synthesis of DHPMs using NiO NPs.



**Scheme 8.** Proposed Mechanism for the synthesis of DHPMs using NiO NPs [211].

all reaction stages, especially under solvent-free conditions, utilizing its Lewis acid and basic sites to activate reactants and facilitate product formation.

### 3. Conclusion

Plant extracts have become a dependable approach for synthesizing nanoparticles because of their safety, environmental friendliness, and cost-effectiveness. The utilization of this environmentally friendly method to synthesise nanoparticles has a wide range of uses in fields such as nanomedicine, pharmaceuticals, cosmetics, environmental science, and the food industry. The high toxicity of traditional methods for NP preparation presents a major challenge, which poses a danger to sectors related to human health. As a result, the scientific community has been continuously looking for novel, secure, and environmentally-friendly methods. In recent decades, there has been significant progress in the production of nanoparticles by biosynthesis, which is considered an environmentally friendly option.

These eco-friendly methods provide exceptional advantages, including as cost-efficiency, environmental compatibility, ease of testing, and lack of toxicity, which make them extremely beneficial for NP synthesis. An additional noteworthy benefit of green synthesis is the use of stability and

reducing chemicals, facilitating convenient regulation of nanoparticle shape and size. NiO NPs are extensively used due to their advantageous features in catalysis, magnetism, antibacterial activity, optics, and photocatalysis. Notably, NiO nanoparticles produced by the use of environmentally benign plant extracts are expected to possess safety, sustainability, and non-harmful properties, rendering them appropriate for diverse applications including catalysis, photocatalysis, and antibacterial purposes.

#### Ethical Approval

This manuscript does not report on or involve the use of any animal or human data or tissue. So the ethical approval is not applicable.

#### Funding

No funding was received to assist with conducting this study and the preparation of this manuscript.

#### Authors Contributions

All authors have contributed equally to prepare the paper.

**Availability of Data and Materials**

There are no associated datasets used in this manuscript.

**Conflict of Interests**

The authors declare that they have no known competing financial interests or personal relationships that could have appeared to influence the work reported in this paper.

**Open Access**

This article is licensed under a Creative Commons Attribution 4.0 International License, which permits use, sharing, adaptation, distribution and reproduction in any medium or format, as long as you give appropriate credit to the original author(s) and the source, provide a link to the Creative Commons license, and indicate if changes were made. The images or other third party material in this article are included in the article's Creative Commons license, unless indicated otherwise in a credit line to the material. If material is not included in the article's Creative Commons license and your intended use is not permitted by statutory regulation or exceeds the permitted use, you will need to obtain permission directly from the OICCPress publisher. To view a copy of this license, visit <https://creativecommons.org/licenses/by/4.0>.

**References**

- [1] A. Bera and H. Belhaj. *J. Nat. Gas Sci. Eng*, **34**:1284–1309, 2016. DOI: <https://doi.org/10.1016/j.jngse.2016.08.023>.
- [2] L.J. Frewer, N. Gupta, S. George, A. Fischer, E. Giles, and D. Coles. *Trends Food Sci. Technol*, **40**:211–225, 2014. DOI: <https://doi.org/10.1016/j.tifs.2014.06.005>.
- [3] L. Syedmoradi, M. Daneshpour, M. Alvandipoura, F.A. Gomez, H. Hajghassem, and K. Omidfar. *Biosens. Bioelectron*, **87**:373–387, 2017. DOI: <https://doi.org/10.1016/j.bios.2016.08.084>.
- [4] B. Eskandari Azar, A. Ramazani, S. Taghavi Fardood, and A. Morsali. *Optik*, **208**:164129, 2019. DOI: <https://doi.org/10.1016/j.ijleo.2019.164129>.
- [5] K. Atrak, A. Ramazani, and S. Taghavi Fardood. *J. Photochem. Photobiol. A: Chem*, **382**:111942, 2019. DOI: <https://doi.org/10.1016/j.jphotochem.2019.111942>.
- [6] S. Taghavi Fardood, F. Moradnia, M. Mostafaei, Z. Afshari, V. Faramarzi, and S. Ganjkanlu. *Nanochem. Res*, **4**:86–93, 2019. DOI: <https://doi.org/10.22036/NCR.2019.01.010>.
- [7] S. Taghavi Fardood, F. Moradnia, and A. Ramazani. *Micro Nano Lett*, **14**:986–991, 2019. DOI: <https://doi.org/10.1049/mnl.2019.0071>.
- [8] A. Swaidan, P. Borthakur, P.K. Boruah, M.R. Das, A. Barras, S. Hamieh, J. Toufaily, T. Hamieh, S. Szunerits, and R. Boukherroub. *Sens. Actuators, B* **294**:253–262, 2019. DOI: <https://doi.org/10.1016/j.snb.2019.05.052>.
- [9] B. Stephen Inbaraj and B.H. Chen. *Biore-sour. Technol*, **102**:8868–8876, 2011. DOI: <https://doi.org/10.1016/j.biortech.2011.06.079>.
- [10] H. Saeidian and F. Moradnia. *Iran. Chem. Commun*, **5**:252–261, 2017.
- [11] B. Karimi, H. Behzadnia, E. Farhangi, E. Jafari, and A. Zamani. *Curr. Org. Synth*, **7**:543–567, 2010. DOI: <https://doi.org/10.2174/157017910794328538>.
- [12] S. Taghavi Fardood, R. Foorotan, F. Moradnia, Z. Afshari, and A. Ramazani. *Mater. Res. Express*, **7**:015086, 2020. DOI: <https://doi.org/10.1088/2053-1591/ab6c8d>.
- [13] F. Moradnia, S. Taghavi Fardood, A. Ramazani, and V. Kumar Gupta. *J. Photochem. Photobiol. A: Chem*, **392**:112433, 2020. DOI: <https://doi.org/10.1016/j.jphotochem.2020.112433>.
- [14] F. Ajormal, F. Moradnia, S. Taghavi Fardood, and A. Ramazani. *J. Chem. Rev*, :90–102, 2020. DOI: <https://doi.org/10.33945/SAMI/JCR.2020.2.2>.
- [15] F. Moradnia, A. Ramazani, S. Taghavi Fardood, and F. Gouranlou. *Mater. Res. Express*, **6**:075057, 2019. DOI: <https://doi.org/10.1088/2053-1591/ab17bc>.
- [16] S. Taghavi Fardood, A. Ramazani, F. Moradnia, Z. Afshari, S. Ganjkanlu, and F. Yekke Zare. *Chem. Method*, **3**:696–706, 2019. DOI: <https://doi.org/10.33945/sami/chemm.2019.6.2>.
- [17] M. A. Bhosale and B. M. Bhanage. *Curr. Org. Chem*, **19**:708–727, 2015. DOI: <https://doi.org/10.2174/1385272819666150207001154>.
- [18] Y. Wang, Z. Xiao, and L. Wu. *Curr. Org. Chem*, **17**:1325–1333, 2013. DOI: <https://doi.org/10.2174/1385272811317120007>.
- [19] H. Batmani, N. Noroozi Pesyan, and F. Havasi. *Microporous Mesoporous Mater*, **257**:27–34, 2018. DOI: <https://doi.org/10.1016/j.micromeso.2017.08.024>.
- [20] N. Noroozi Pesyan, H. Batmani, and F. Havasi. *Polyhedron*, **158**:248–254, 2019. DOI: <https://doi.org/10.1016/j.poly.2018.11.005>.
- [21] K. Atrak, A. Ramazani, and S. Taghavi Fardood. *Environ. Technol*, **41**:2760–2770, 2019. DOI: <https://doi.org/10.1080/09593330.2019.1581841>.

- [22] S. Wen, T. Yang, N. Zhao, L. Ma, and E. Liu. *Appl. Catal*, **B 258**:117953, 2019. DOI: <https://doi.org/10.1016/j.apcatb.2019.117953>.
- [23] L. Ouni, A. Ramazani, and S. Taghavi Fardood. *Front. Chem. Sci. Eng*, **13**:274–295, 2019. DOI: <https://doi.org/10.1007/s11705-018-1765-0>.
- [24] S. Taghavi Fardood, F. Moradnia, S. Moradi, R. Foroootan, F. Yekke Zare, and M. Heidari. *Nanochem. Res*, **4**:140–147, 2019. DOI: <https://doi.org/10.22036/ncr.2019.02.005>.
- [25] B. Wang, S. He, L. Zhang, X. Huang, F. Gao, W. Feng, and P. Liu. *Appl. Catal*, **B 243**:229–235, 2019. DOI: <https://doi.org/10.1016/j.apcatb.2018.10.065>.
- [26] E. Pourtaheri, M.A. Taher, G.A. Ali, S. Agarwal, and V.K. Gupta. *Int. J. Electrochem. Sci*, **14**:9622–9632, 2019. DOI: <https://doi.org/10.20964/2019.10.01>.
- [27] A. Kumar, B. Paul, R. Boukherroub, and S.L. Jain. *J. Hazard. Mater*, :121700, 2019. DOI: <https://doi.org/10.1016/j.jhazmat.2019.121700>.
- [28] L.J. Hazeem, G. Kuku, E. Dewailly, C. Slomianny, A. Barras, A. Hamdi, R. Boukherroub, M. Culha, and M. Bououdina. *Nanomaterials*, **9**:914, 2019. DOI: <https://doi.org/10.3390/nano9070914>.
- [29] R. Kumar, B.S. Inbaraj, and B. Chen. *Mater. Res. Bull*, **45**:1603–1607, 2010. DOI: <https://doi.org/10.1016/j.materresbull.2010.07.017>.
- [30] H. Saeidian, S.V. Khajeh, Z. Mirjafary, and B. Eftekhari-Sis. *RSC Adv*, **8**:38801–38807, 2018. DOI: <https://doi.org/10.1039/C8RA08376B>.
- [31] S. Mallakpour and M. Madani. *Prog. Org. Coat*, **86**:194–207, 2015. DOI: <https://doi.org/10.1016/j.porgcoat.2015.05.023>.
- [32] M. Sundrarajan, S. Ambika, and K. Bharathi. *Adv. Powder Technol*, **26**:1294–1299, 2015. DOI: <https://doi.org/10.1016/j.appt.2015.07.001>.
- [33] V. Thirumalai Arasu, D. Prabhu, and M. Soniya. *J. Bio. Sci. Res*, **1**:259–270, 2010.
- [34] R. Varshney, S. Bhadauria, and M.S. Gaur. *Nano Biomed. Eng*, **4**:99–106, 2012. DOI: <https://doi.org/10.5101/nbe.v4i2.p99-106>.
- [35] S. Suresh. *Nanotechnol*, **3**:62–74, 2013.
- [36] N. Rajput. *Int. J. Adv. Eng. Tech*, **7**:1806, 2015.
- [37] G. Vitor, T. Palma, B. Vieira, J. Lourenco, R. Barros, and M.C. Costa. *Miner. Eng*, **75**:85–93, 2015. DOI: <https://doi.org/10.1016/j.mineng.2014.12.003>.
- [38] F. Karampour. *Asian J. Green Chem*, **7**:149–162, 2023. DOI: <https://doi.org/10.22034/ajgc.2023.394268.1384>.
- [39] N. Pourbahar and S. Sattari Alamdar. *Asian J. Green Chem*, **7**:9–16, 2023. DOI: <https://doi.org/10.22034/ajgc.2023.1.2>.
- [40] O.K. Awote, O.S. Anagun, A.G. Adeyemo, J.O. Igbalaye, M.L. Ogunc, S.K. Apete, S.O. Folami, F.E. Olalero, S.C. Ebube, M.I. Taofeeq, and O.O. Akinloye. *Asian J. Green Chem*, **6**:284–296, 2022. DOI: <https://doi.org/10.22034/ajgc.2022.4.1>.
- [41] M.I. Rashid, T. Shahzad, M. Shahid, I.M. Ismail, G.M. Shah, and T. Almeelbi. *J. Hazard. Mater*, **324**:298–305, 2017. DOI: <https://doi.org/10.1016/j.jhazmat.2016.10.063>.
- [42] R. Shaikh, J. Nayab, and N. Shaikh. *Asian J. Green Chem*, **5**:313–324, 2021. DOI: <https://doi.org/10.22034/ajgc.2021.284592.1302>.
- [43] N.M. Nemma and Z.S. Sadeq. *Chem. Method*, **7**:325–334, 2023. DOI: <https://doi.org/10.22034/chemm.2023.381408.1646>.
- [44] C. Vidya, S. Hiremath, M. Chandraprabha, M.L. Antonyraj, I.V. Gopal, A. Jain, and K. Bansal. *Int J Curr Eng Technol*, **1**:118–120, 2013.
- [45] R. Aladpoosh and M. Montazer. *Carbohydr. Polym*, **126**:122–129, 2015. DOI: <https://doi.org/10.1016/j.carbpol.2015.03.036>.
- [46] M.T. Swihart. *Curr. Opin. Colloid Interface Sci*, **8**:127–133, 2003. DOI: [https://doi.org/10.1016/S1359-0294\(03\)00007-4](https://doi.org/10.1016/S1359-0294(03)00007-4).
- [47] N.A. Patil, S. Udgire, D.R. Shinde, and P.D. Patil. *Chem. Method*, **7**:15–27, 2023. DOI: <https://doi.org/10.22034/chemm.2023.355289.1597>.
- [48] R. Yuvakkumar, J. Suresh, B. Saravanakumar, A.J. Nathanael, S.I. Hong, and V. Rajendran. *Spectrochim. Acta, Part A*, **137**:250–258, 2015. DOI: <https://doi.org/10.1016/j.saa.2014.08.022>.
- [49] C. Tan and H. Zhang. *Nat. Commun*, **6**:7873, 2015. DOI: <https://doi.org/10.1038/ncomms8873>.
- [50] R. Laine, J. Marchal, H. Sun, and X. Pan. *Nat. Mater*, **5**:710, 2006. DOI: <https://doi.org/10.1038/nmat1711>.
- [51] F. Foroughi, S. Hassanzadeh-Tabrizi, and J. Amighian. *J. Magn. Magn. Mater*, **382**:182–187, 2015. DOI: <https://doi.org/10.1016/j.jmmm.2015.01.075>.
- [52] F. Liu, X. He, J. Zhang, H. Chen, H. Zhang, and Z. Wang. *J. Mater. Chem. B*, **3**:6731–6739, 2015. DOI: <https://doi.org/10.1039/C5TB01159K>.
- [53] J.-H. Noh and R. Meijboom. *Appl. Catal., A*, **497**:107–120, 2015. DOI: <https://doi.org/10.1016/j.apcata.2015.02.039>.



- [54] S. Taghavi Fardood, F. Moradnia, R. Forootan, R. Abbassi, S. Jalalifar, A. Ramazani, and M. Sillanpaa. *J. Photochem. Photobiol. A: Chem*, **423**:113621, 2022. DOI: <https://doi.org/10.1016/j.jphotochem.2021.113621>.
- [55] S.M. Khoshfetrat, K. Fasihi, F. Moradnia, H.K. Zaidan, and E. Sanchooli. *Anal. Chim. Acta*, **1252**:341073, 2023. DOI: <https://doi.org/10.1016/j.aca.2023.341073>.
- [56] P. Dhandapani, A.S. Siddarth, S. Kamalasekaran, S. Maruthamuthu, and G. Rajagopal. *Carbohydr. Polym*, **103**:448–455, 2014. DOI: <https://doi.org/10.1016/j.carbpol.2013.12.074>.
- [57] C. Dhand, N. Dwivedi, X.J. Loh, A.N.J. Ying, N.K. Verma, R.W. Beuerman, R. Lakshminarayanan, and S. Ramakrishna. *RSC Adv*, **5**:105003–105037, 2015. DOI: <https://doi.org/10.1039/C5RA19388E>.
- [58] M. Sadat-Shojai, M.-T. Khorasani, E. Dinpanah-Khoshdargi, and A. Jamshidi. *Acta Biomater*, **9**:7591–7621, 2013. DOI: <https://doi.org/10.1016/j.actbio.2013.04.012>.
- [59] F. Moradnia, S. Taghavi Fardood, A. Ramazani, B. k. Min, S.W. Joo, and R.S. Varma. *J. Cleaner Prod*, **288**:125632, 2021. DOI: <https://doi.org/10.1016/j.jclepro.2020.125632>.
- [60] F. Ali, S. Akbar, M. Sillanpaa, U. Younas, A. Ashraf, M. Pervaiz, R. Kausar, I. Ahmad, A.A. Alothman, and M. Ouladsmane. *Chemosphere*, **313**:137321, 2022. DOI: <https://doi.org/10.1016/j.chemosphere.2022.137321>.
- [61] Y. Li S. Frindy and M. Sillanpää. *Sep. Purif. Technol*, **284**:120241, 2022. DOI: <https://doi.org/10.1016/j.seppur.2021.120241>.
- [62] K. Atrak, A. Ramazani, and S. Taghavi Fardood. *J. Mater. Sci. Mater. Electron*, **29**:8347–8353, 2018. DOI: <https://doi.org/10.1007/s10854-018-8845-2>.
- [63] S. Taghavi Fardood, A. Ramazani, and S.W. Joo. *J. Appl. Chem. Res*, **12**:8–15, 2018.
- [64] H. Bar, D.K. Bhui, G.P. Sahoo, P. Sarkar, S.P. De, and A. Misra. *Colloids Surf. Physicochem. Eng. Aspects*, **339**:134–139, 2009. DOI: <https://doi.org/10.1016/j.colsurfa.2009.02.008>.
- [65] F. Thema, P. Beukes, A. Gurib-Fakim, and M. Maaza. *J. Alloys Compd*, **646**:1043–1048, 2015. DOI: <https://doi.org/10.1016/j.jallcom.2015.05.279>.
- [66] D. Philip. *Spectrochim. Acta, Part A*, **73**:650–653, 2009. DOI: <https://doi.org/10.1016/j.saa.2009.03.007>.
- [67] V.G. Kumar, S.D. Gokavarapu, A. Rajeswari, T.S. Dhas, V. Karthick, Z. Kapadia, T. Shrestha, I. Barathy, A. Roy, and S. Sinha. *Colloids Surf. B. Biointerfaces*, **87**:159–163, 2011. DOI: <https://doi.org/10.1016/j.colsurfb.2011.05.016>.
- [68] T. Sun, Z. Zhang, J. Xiao, C. Chen, F. Xiao, S. Wang, and Y. Liu. *Sci. Rep*, **3**:2527, 2013. DOI: <https://doi.org/10.1038/srep02527>.
- [69] S. Jain and M.S. Mehata. *Sci. Rep*, **7**:15867, 2017. DOI: <https://doi.org/10.1038/s41598-017-15724-8>.
- [70] S. Irvani. *Green Chem*, **13**:2638–2650, 2011. DOI: <https://doi.org/10.1039/C1GC15386B>.
- [71] S. Taghavi Fardood, Z. Hosseinzadeh, and A. Ramazani. *Chem. Method*, **8**:154–163, 2024. DOI: <https://doi.org/10.48309/chemm.2024.430664.1748>.
- [72] D. Suresh, P. Nethravathi, H. Rajanaika, H. Nagabhushana, and S. Sharma. *Sci. Semicond. Process*, **31**:446–454, 2015. DOI: <https://doi.org/10.1016/j.mssp.2014.12.023>.
- [73] S. Taghavi Fardood, F. Moradnia, A.H. Ghalaichi, S. Danesh Pajouh, and M. Heidari. *Nanochem. Res*, **5**:69–76, 2020. DOI: <https://doi.org/10.22036/ncr.2020.01.007>.
- [74] F. Moradnia, S. Taghavi Fardood, A. Ramazani, S. Osali, and I. Abdolmaleki. *Micro Nano Lett*, **15**:674–677, 2020. DOI: <https://doi.org/10.1049/mnl.2020.0189>.
- [75] R.G. Saratale, G.D. Saratale, H.S. Shin, J.M. Jacob, A. Pugazhendhi, M. Bhaisare, and G. Kumar. *Environ. Sci. Pollut. Res*, **25**:10164–10183, 2018. DOI: <https://doi.org/10.1007/s11356-017-9912-6>.
- [76] P. Vanathi, P. Rajiv, S. Narendhran, S. Rajeshwari, P.K. Rahman, and R. Venckatesh. *Mater. Lett*, **134**:13–15, 2014. DOI: <https://doi.org/10.1016/j.matlet.2014.07.029>.
- [77] P. Jamdagni, P. Khatri, and J. Rana. *J. King Saud Univ. Sci*, **30**:168–175, 2018. DOI: <https://doi.org/10.1016/j.jksus.2016.10.002>.
- [78] K. Prasad and A.K. Jha. *Nat. Sci*, **1**:129, 2009. DOI: <https://doi.org/10.4236/ns.2009.12016>.
- [79] B.N. Patil and T.C. Taranath. *Int. J. Mycobacteriol*, **5**:197–204, 2016. DOI: <https://doi.org/10.1016/j.ijmyco.2016.03.004>.
- [80] S. Gunalan, R. Sivaraj, and V. Rajendran. *Prog. Nat. Sci-Mater*, **22**:693–700, 2012. DOI: <https://doi.org/10.1016/j.pnsc.2012.11.015>.
- [81] J. Guo, S. Zhu, Z. Chen, Y. Li, Z. Yu, Q. Liu, J. Li, C. Feng, and D. Zhang. *Ultrason. Sonochem*, **18**:1082–1090, 2011. DOI: <https://doi.org/10.1016/j.ultsonch.2011.03.021>.
- [82] N. Sofyan, A. Ridhova, A.H. Yuwono, A. Udhiarto, and J.W. Fergus. *Int. J. Energy Res*, **43**:5959–5968, 2019. DOI: <https://doi.org/10.1002/er.4710>.

- [83] S.D. Henam, F. Ahmad, M.A. Shah, S. Parveen, and A.H. Wani. *Spectrochim. Acta, Part A*, **213**:337–341, 2019. DOI: <https://doi.org/10.1016/j.saa.2019.01.071>.
- [84] N. Silva, S. Ramírez, I. Díaz, A. Garcia, and N. Hassan. *Mater.*, **12**:804, 2019. DOI: <https://doi.org/10.3390/ma12050804>.
- [85] S.R. Christy, L.S. Priya, M. Durka, A. Dinsh, N. Babitha, and S. Arunadevi. *J. Nanosci. Nanotechnol.*, **19**:3564–3570, 2019. DOI: <https://doi.org/10.1166/jnn.2019.16141>.
- [86] N.A.A. Yusof, N.M. Zain, and N. Pauzi. *Int. J. Biol. Macromol.*, **124**:1132–1136, 2019. DOI: <https://doi.org/10.1016/j.ijbiomac.2018.11.228>.
- [87] B.A. Abbasi, J. Iqbal, T. Mahmood, R. Ahmad, S. Kanwal, and S. Afridi. *Mater. Res. Express*, **6**:0850a0857, 2019. DOI: <https://doi.org/10.1088/2053-1591/ab23e1>.
- [88] J. Xu, M. Wang, Y. Liu, J. Li, and H. Cui. *Adv. Powder Technol.*, **30**:861–868, 2019. DOI: <https://doi.org/10.1016/j.apt.2019.01.016>.
- [89] C. Jayaseelan, A.A. Rahuman, A.V. Kirthi, S. Marimuthu, T. Santhoshkumar, A. Bagavan, K. Gaurav, L. Karthik, and K.B. Rao. *Spectrochim. Acta, Part A*, **90**:78–84, 2012. DOI: <https://doi.org/10.1016/j.saa.2012.01.006>.
- [90] A.E. Angel, J.V. Judith, K. Kaviyarasu, L.K. John, R. Ramalingam, and H. Al-Lohedan. *J. Photochem. Photobiol. B: Biol.*, **180**:39–50, 2018. DOI: <https://doi.org/10.1016/j.jphotobiol.2018.01.023>.
- [91] A. Diallo, K. Kaviyarasu, S. Ndiaye, B. Mothudi, V. Rajendran A. Ishaq, and M. Maaza. *Green Chem. Lett. Rev.*, **11**:166–175, 2018. DOI: <https://doi.org/10.1080/17518253.2018.1447604>.
- [92] S. Ravikumar, R. Gokulakrishnan, and P. Boomi. *Asian Pac. J.Trop. Dis.*, **2**:85–89, 2012. DOI: [https://doi.org/10.1016/S2222-1808\(12\)60022-X](https://doi.org/10.1016/S2222-1808(12)60022-X).
- [93] M.I. Din, A.G. Nabi, A. Rani, A. Aihetasham, M. Mukhtar, and Environ. *Nanotechnol. Monit. Manage.*, **9**:29–36, 2018. DOI: <https://doi.org/10.1016/j.enmm.2017.11.005>.
- [94] M.G. Berhe and Y.T. Gebreslassie. *Int. J. Nanomed.*, **18**:4229–4251, 2023. DOI: <https://doi.org/10.2147/IJN.S410668>.
- [95] E.S. Mehr, M. Sorbiun, A. Ramazani, and S. Taghavi Fardood. *J. Mater. Sci. Mater. Electron*, **29**:1333–1340, 2018. DOI: <https://doi.org/10.1007/s10854-017-8039-3>.
- [96] S. Taghavi Fardood and A. Ramazani. *J. Appl. Chem. Res.*, **12**:8–15, 2018.
- [97] S. Ahmed, M. Ahmad, B.L. Swami, and S. Ikram. *J. Adv. Res.*, **7**:17–28, 2016. DOI: <https://doi.org/10.1016/j.jare.2015.02.007>.
- [98] S. Taghavi Fardood, A. Ramazani, P.A. Asiabi, and S.W. Joo. *J. Struct. Chem.*, **59**:1737–1743, 2018. DOI: <https://doi.org/10.1134/s0022476618070302>.
- [99] M.T. Kiani, A. Ramazani, S. Rahmani, and S. Taghavi Fardood. *Int. J. Environ. Anal. Chem.*, **30**:1–17, 2022. DOI: <https://doi.org/10.1080/03067319.2022.2076219>.
- [100] A.A. Mariam, M. Kashif, S. Arokiyaraj, M. Bououdina, M. Sankaracharyulu, M. Jayachandran, and U. Hashim. *Dig. J. Nanomater. Biostruct.*, **9**:1007–1019, 2014.
- [101] B. Sone, X. Fuku, and M. Maaza. *Int J Electrochem Sci*, **11**:8204–8220, 2016. DOI: <https://doi.org/10.20964/2016.10.17>.
- [102] M. Heinlaan, A. Ivask, I. Blinova, H.-C. Dubourguier, and A. Kahru. *Chemosphere*, **71**:1308–1316, 2008. DOI: <https://doi.org/10.1016/j.chemosphere.2007.11.047>.
- [103] J. Qu, X. Yuan, X. Wang, and P. Shao. *Environ. Pollut.*, **159**:1783–1788, 2011. DOI: <https://doi.org/10.1016/j.envpol.2011.04.016>.
- [104] P. Korde, S. Ghotekar, T. Pagar, S. Pansambal, R. Oza, and D. Mane. *J. Chem. Rev.*, **2**:157–168, 2020. DOI: <https://doi.org/10.22034/jcr.2020.106601>.
- [105] Y. Singh, R.S. Sodhi, P.P. Singh, and S. Kaushal. *Materials Advances*, **3**:4991–5000, 2022. DOI: <https://doi.org/10.1039/D2MA00114D>.
- [106] P. Kganyago, L. Mahlaule-Glory, M. Mathipa, B. Ntsendwana, N. Mketso, Z. Mbita, and N. Hintsho-Mbita. *J. Photochem. Photobiol. B: Biol.*, **182**:18–26, 2018. DOI: <https://doi.org/10.1016/j.jphotobiol.2018.03.016>.
- [107] A.T. Khalil, M. Ovais, I. Ullah, M. Ali, Z.K. Shinwari, D. Hassan, and M. Maaza. *Artificial cells, nanomedicine, and biotechnology*, **46**:838–852, 2018. DOI: <https://doi.org/10.1080/21691401.2017.1345928>.
- [108] M. Kundu, G. Karunakaran, and D. Kuznetsov. *Powder Technol.*, **311**:132–136, 2017. DOI: <https://doi.org/10.1016/j.powtec.2017.01.085>.
- [109] N. Behera, M. Arakha, M. Priyadarshinee, B.S. Pattanayak, S. Soren, S. Jha, and B.C. Mallick. *RSC Adv.*, **9**:24888–24894, 2019. DOI: <https://doi.org/10.1039/C9RA02082A>.
- [110] S. Taghavi Fardood, A. Ramazani, and S. Moradi. *Chem. J. Mold*, **12**:115–118, 2017. DOI: <https://doi.org/10.19261/cjm.2017.383>.

- [111] A.A. Ezhilarasi, J.J. Vijaya, K. Kaviyarasu, M. Maaza, A. Ayeshamariam, and L.J. Kennedy. *J. Photochem. Photobiol. B: Biol.*, **164**:352–360, 2016. DOI: <https://doi.org/10.1016/j.jphotobiol.2016.10.003>.
- [112] X. Fuku, N. Matinise, M. Masikini, K. Kasinathan, and M. Maaza. *Mater. Res. Bull.*, **97**:457–465, 2018. DOI: <https://doi.org/10.1016/j.materresbull.2017.09.022>.
- [113] M. Nasserri, F. Ahrari, and B. Zakerinasab. *Appl. Organomet. Chem.*, **30**:978–984, 2016. DOI: <https://doi.org/10.1002/aoc.3530>.
- [114] B.M. Escobar, M.G. Lucio, R. Barbosa, and D.A. Morales. Synthesis and characterization of nio nanoparticles using manihot esculenta aqueous extracts. In *Preprints*. 2018. DOI: <https://doi.org/10.20944/preprints201811.0242.v1>.
- [115] S. Saleem, B. Ahmed, M.S. Khan, M. Al-Shaeri, and J. Musarrat. *Microb. Pathog.*, **111**:375–387, 2017. DOI: <https://doi.org/10.1016/j.micpath.2017.09.019>.
- [116] J. Sharma, P. Srivastava, G. Singh, M.S. Akhtar, and S. Ameen. *Ceram. Int.*, **41**:1573–1578, 2015. DOI: <https://doi.org/10.1016/j.ceramint.2014.09.093>.
- [117] S. Sudhasree, A. Shakila Banu, P. Brindha, and G.A. Kurian. *Toxicol. Environ. Chem.*, **96**:743–754, 2014. DOI: <https://doi.org/10.1080/02772248.2014.923148>.
- [118] F. Thema, E. Manikandan, A. Gurib-Fakim, and M. Maaza. *J. Alloys Compd.*, **657**:655–661, 2016. DOI: <https://doi.org/10.1016/j.jallcom.2015.09.227>.
- [119] R. Yuvakkumar, J. Suresh, A.J. Nathanael, M. Sundrarajan, and S. Hong. *Mater. Lett.*, **128**:170–174, 2014. DOI: <https://doi.org/10.1016/j.matlet.2014.04.112>.
- [120] M.S. Kumar, T. Soundarya, G. Nagaraju, G. Raghu, N. Rekha, F.A. Alharthi, and B. Nirmala. *Inorg. Chim. Acta*, **515**:120059, 2021. DOI: <https://doi.org/10.1016/j.ica.2020.120059>.
- [121] R. Ramesh, V. Yamini, S.J. Sundaram, F.L.A. Khan, and K. Kaviyarasu. *Mater. Today: Proc.*, **36**:268–272, 2021. DOI: <https://doi.org/10.1016/j.matpr.2020.03.581>.
- [122] D. Deepthi, B.S. Rahman, M. Senthilkumar, S. Paranthaman, J. Ahamed, and S.B. Bathusha. *J. pharmacogn. phytochem.*, **10**:20–28, 2021.
- [123] N. Al-Zaqri, K. Umamakeshvari, V. Mohana, A. Muthuvel, and A. Boshala. *J. Mater. Sci. Mater. Electron.*, **33**:11864–11880, 2022. DOI: <https://doi.org/10.1007/s10854-022-08149-1>.
- [124] M. Boudiaf, Y. Messai, E. Bentouhami, M. Schmutz, C. Blanck, L. Ruhlmann, H. Bezzi, L. Tairi, and D.E. Mekki. *J. Phys. Chem. Solids*, **153**:110020, 2021. DOI: <https://doi.org/10.1016/j.jpcs.2021.110020>.
- [125] I.M. Rashid, S.D. Salman, A.K.M. Mahdi, and Y. Salih. *Sains Malays.*, **51**:533–546, 2022. DOI: <https://doi.org/10.17576/jsm-2022-5102-17>.
- [126] M. Mahadevaswamy, S.R. Paniyadi, A. Lakshmikanthan, S.A. Swamirayachar, M.P.G. Chandrashekarappa, K. Giasin, V.K. Shivaraju, M.B. Chougala, and E. Linul. *J. Mater. Res. Technol.*, **19**:4543–4556, 2022. DOI: <https://doi.org/10.1016/j.jmrt.2022.06.166>.
- [127] Z.T. Khodair, N.M. Ibrahim, T.J. Kadhim, and A.M. Mohammad. *Chem. Phys. Lett.*, **797**:139564, 2022. DOI: <https://doi.org/10.1016/j.cplett.2022.139564>.
- [128] A. Singh, V. Goyal, J. Singh, H. Kaur, S. Kumar, K.M. Batoo, J. Gaur, M. Pal, M. Rawat, and S. Hussain. *J. Cleaner Prod.*, **343**:131026, 2022. DOI: <https://doi.org/10.1016/j.jclepro.2022.131026>.
- [129] B. Ahmad, M. Khan, M. Naeem, A. Alhodaib, M. Fatima, M. Amami, E.A. Al-Abbad, A. Kausar, N. Alwadai, and A. Nazir. *Mater. Chem. Phys.*, page 126363, 2022. DOI: <https://doi.org/10.1016/j.matchemphys.2022.126363>.
- [130] I. Mamonova, I. Babushkina, I. Norkin, E. Gladkova, M. Matasov, and D. Puchin'yan. *Nanotechnologies Russ.*, **10**:128–134, 2015. DOI: <https://doi.org/10.1134/S1995078015010139>.
- [131] A. Zarei, S. Taghavi Fardood, F. Moradnia, and A. Ramazani. *Eurasian Chem. Commun.*, **2**:798–811, 2020. DOI: <https://doi.org/10.33945/SAMI/ECC.2020.7.7>.
- [132] A.A. Ezhilarasi, J.J. Vijaya, K. Kaviyarasu, L.J. Kennedy, R.J. Ramalingam, and H.A. Al-Lohedan. *J. Photochem. Photobiol. B: Biol.*, **180**:39–50, 2018. DOI: <https://doi.org/10.1016/j.jphotobiol.2018.01.023>.
- [133] T. Kavitha and H. Yuvaraj. *J. Mater. Chem.*, **21**:15686–15691, 2011. DOI: <https://doi.org/10.1039/C1JM13278D>.
- [134] P.I. Rajan, J.J. Vijaya, S. Jesudoss, K. Kaviyarasu, L.J. Kennedy, R. Jothiramalingam, H.A. Al-Lohedan, and M.-A. Vaali-Mohammed. *Mater. Res. Express*, **4**:085030, 2017. DOI: <https://doi.org/10.1088/2053-1591/aa7e3c>.
- [135] B. Shanaj and X. John. *J. Theor. Comput. Sci.*, **3**:149–159, 2016. DOI: <https://doi.org/10.4172/2376-130X.1000149>.
- [136] S. Chaudhary, Y. Kaur, B. Jayee, G.R. Chaudhary, and A. Umar. *J. Cleaner Prod.*, **190**:563–576, 2018. DOI: <https://doi.org/10.1016/j.jclepro.2018.04.110>.

- [137] V. Helan, J.J. Prince, N.A. Al-Dhabi, M.V. Arasu, A. Ayeshamariam, G. Madhumitha, S.M. Roopan, and M. Jayachandran. *Results Phys.*, **6**:712–718, 2016. DOI: <https://doi.org/10.1016/j.rinp.2016.10.005>.
- [138] K.S. Khashan, G.M. Sulaiman, A.H. Hamad, F.A. Abdulameer, and A. Hadi. *Appl. Phys. A*, **123**:190, 2017. DOI: <https://doi.org/10.1007/s00339-017-0826-4>.
- [139] V. Benitha, K. Jeyasubramanian, R. Mala, G. Hikku, and R.R. Kumar. *J. Coat. Technol. Res.*, **16**:59–70, 2019. DOI: <https://doi.org/10.1007/s11998-018-0100-5>.
- [140] S.A. Bhat, F. Zafar, A.H. Mondal, A. Kareem, A.U. Mirza, S. Khan, A. Mohammad, Q.M.R. Haq, and N. Nishat. *J. Iran. Chem. Soc.*, **17**:215–227, 2020. DOI: <https://doi.org/10.1007/s13738-019-01767-3>.
- [141] K. Kannan, D. Radhika, M.P. Nikolova, K.K. Sadasivuni, H. Mahdizadeh, and U. Verma. *Inorg. Chem. Commun.*, **113**:107755, 2020. DOI: <https://doi.org/10.1016/j.inoche.2019.107755>.
- [142] L. Umaralikhan and M.J.M. Jaffar. *J. Adv. Appl. Sci. Res.*, **1**:24–35, 2016. DOI: <https://doi.org/10.46947/joaasr14201628>.
- [143] N. Talebian, M. Doudi, and M. Kheiri. *J. Sol-Gel Sci. Technol.*, **69**:172–182, 2014. DOI: <https://doi.org/10.1007/s10971-013-3201-8>.
- [144] D. Amantini, R. Beleggia, F. Fringuelli, F. Pizzo, and L. Vaccaro. *J. Org. Chem.*, **69**:2896–2898, 2004. DOI: <https://doi.org/10.1021/jo0499468>.
- [145] J. Iqbal, B.A. Abbasi, T. Mahmood, S. Hameed, A. Munir, and S. Kanwal. *Appl. Organomet. Chem.*, **33**:e4950, 2019. DOI: <https://doi.org/10.1002/aoc.4950>.
- [146] D. Paul and S. Neogi. *Mater. Res. Express*, **6**:055004, 2019. DOI: <https://doi.org/10.1088/2053-1591/ab003c>.
- [147] Z. Wang, Y.-H. Lee, B. Wu, A. Horst, Y. Kang, Y.J. Tang, and D.-R. Chen. *Chemosphere*, **80**:525–529, 2010. DOI: <https://doi.org/10.1016/j.chemosphere.2010.04.047>.
- [148] M. Rezaei and A. Nezamzadeh-Ejhiha. *Int. J. Hydrogen Energy*, **45**:24749–24764, 2020. DOI: <https://doi.org/10.1016/j.ijhydene.2020.06.258>.
- [149] S. Taghavi Fardood, F. Moradnia, S. Heidarzadeh, and A. Naghipour. *Nanochem. Res.*, **8**:134, 2023. DOI: <https://doi.org/10.22036/ncr.2023.02.006>.
- [150] H. Derikvandi and A. Nezamzadeh-Ejhih. *J. Colloid Interface Sci.*, **490**:314–327, 2017. DOI: <https://doi.org/10.1016/j.jcis.2016.11.069>.
- [151] S. Senobari and A. Nezamzadeh-Ejhih. *J. Mol. Liq.*, **261**:208–217, 2018. DOI: <https://doi.org/10.1016/j.molliq.2018.04.028>.
- [152] A. Houas, H. Lachheb, M. Ksibi, E. Elaloui, C. Guillard, and J.-M. Herrmann. *Appl. Catal., B*, **31**:145–157, 2001. DOI: [https://doi.org/10.1016/S0926-3373\(00\)00276-9](https://doi.org/10.1016/S0926-3373(00)00276-9).
- [153] Y. Zhang, Y. Liu, C. Ge, H. Yin, M. Ren, A. Wang, T. Jiang, and L. Yu. *Powder Technol.*, **192**:171–177, 2009. DOI: <https://doi.org/10.1016/j.powtec.2008.12.009>.
- [154] S.A. Ansari, M.M. Khan, S. Kalathil, A. Nisar, J. Lee, and M.H. Cho. *Nanoscale*, **5**:9238–9246, 2013. DOI: <https://doi.org/10.1039/C3NR02678G>.
- [155] K.V.S. Rao, A. Rachel, M. Subrahmanyam, and P. Boule. *Appl. Catal., B*, **46**:77–85, 2003. DOI: [https://doi.org/10.1016/S0926-3373\(03\)00199-1](https://doi.org/10.1016/S0926-3373(03)00199-1).
- [156] S. Zahmatkesh, A. Bokhari, M. Karimian, M.M.A. Zahra, M. Sillanpää, H. Panchal, A.J. Alrubaie, and Y. Rezakhani. *Environ. Monit. Assess.*, **194**:1–15, 2022. DOI: <https://doi.org/10.1007/s10661-022-10503-z>.
- [157] Z. Hu, Y. Zhang, L. Pu, B. Wang, S. Yang, and H. Li. *J. Cleaner Prod.*, **377**:134423, 2022. DOI: <https://doi.org/10.1016/j.jclepro.2022.134423>.
- [158] S. Senobari and A. Nezamzadeh-Ejhih. *J. Mol. Liq.*, **257**:173–183, 2018. DOI: <https://doi.org/10.1016/j.molliq.2018.02.096>.
- [159] L. Xu, L.-P. Jiang, and J.-J. Zhu. *Nanotechnology*, **20**:045605, 2008. DOI: <https://doi.org/10.1088/0957-4484/20/4/045605>.
- [160] C. Wang, X. Wang, B.-Q. Xu, J. Zhao, B. Mai, G. Sheng, and J. Fu. *J. Photochem. Photobiol. A: Chem.*, **168**:47–52, 2004. DOI: <https://doi.org/10.1016/j.jphotochem.2004.05.014>.
- [161] S. Kaizra, Y. Louafi, B. Bellal, M. Trari, and G. Rekhila. *Mater. Sci. Semicond. Process.*, **30**:554–560, 2015. DOI: <https://doi.org/10.1016/j.mssp.2014.10.045>.
- [162] Z.U. Khan, M. Moronshing, M. Shestakova, A. Al-Othman, M. Sillanpää, Z. Zhan, B. Song, and Y. Lei. *Desalination*, **548**:116254, 2023. DOI: <https://doi.org/10.1016/j.desal.2022.116254>.
- [163] M.S. Bashir, C. Zhou, C. Wang, M. Sillanpää, and F. Wang. *Sep. Purif. Technol.*, **304**:122307, 2023. DOI: <https://doi.org/10.1016/j.seppur.2022.122307>.
- [164] M. Karimi-Shamsabadi, M. Behpour, A.K. Babaheidari, and Z. Saberi. *J. Photochem. Photobiol. A: Chem.*, **346**:133–143, 2017. DOI: <https://doi.org/10.1016/j.jphotochem.2017.05.038>.



- [165] F. Iazdani and A. Nezamzadeh-Ejhieh. *Spectrochim. Acta, Part A*, **250**:119228, 2021. DOI: <https://doi.org/10.1016/j.saa.2020.119228>.
- [166] N.A. Khan, K. Saeed, I. Khan, T. Gul, M. Sadiq, A. Uddin, and I. Zekker. *Appl. Water Sci.*, **12**:131, 2022. DOI: <https://doi.org/10.1007/s13201-022-01647-x>.
- [167] F. Fazlali, A. Mahjoub, and R. Abazari. *Solid State Sci.*, **48**:263–269, 2015. DOI: <https://doi.org/10.1016/j.solidstatesciences.2015.08.022>.
- [168] K. Karthik, M. Shashank, V. Revathi, and T. Tatarchuk. *Mol. Cryst. Liq. Cryst.*, **673**:70–80, 2018. DOI: <https://doi.org/10.1080/15421406.2019.1578495>.
- [169] F. Motahari, M.R. Mozdianfard, F. Soofivand, and M. Salavati-Niasari. *RSC Adv.*, **4**:27654–27660, 2014. DOI: <https://doi.org/10.1039/C4RA02697G>.
- [170] M. Ramesh, M.P.C. Rao, S. Anandan, and H. Nagaraja. *J. Mater. Res.*, **33**:601–610, 2018. DOI: <https://doi.org/10.1557/jmr.2018.30>.
- [171] W. Sun, L. Xiao, and X. Wu. *J. Alloys Compd.*, **772**:465–471, 2019. DOI: <https://doi.org/10.1016/j.jallcom.2018.09.185>.
- [172] R. Vahini, P.S. Kumar, and S. Karuthapan-dian. *Appl. Phys. A*, **122**:744, 2016. DOI: <https://doi.org/10.1007/s00339-016-0277-3>.
- [173] L. Zhang, L. An, B. Liu, and H. Yang. *Appl. Phys. A*, **104**:69, 2011. DOI: <https://doi.org/10.1007/s00339-011-6403-3>.
- [174] Q. Dong, S. Yin, C. Guo, X. Wu, N. Kumada, T. Takei, A. Miura, Y. Yonesaki, and T. Sato. *Appl. Catal., B*, **147**:741–747, 2014. DOI: <https://doi.org/10.1016/j.apcatb.2013.10.007>.
- [175] K. Hayat, M. Gondal, M.M. Khaled, and S. Ahmed. *J. Mol. Catal. A: Chem.*, **336**:64–71, 2011. DOI: <https://doi.org/10.1016/j.molcata.2010.12.011>.
- [176] C. Pan, R. Ding, Y. Hu, and G. Yang. *Physica E Low Dimens. Syst. Nanostruct.*, **54**:138–143, 2013. DOI: <https://doi.org/10.1016/j.physe.2013.05.021>.
- [177] S. Shang, K. Xue, D. Chen, and X. Jiao. *CrystEngComm*, **13**:5094–5099, 2011. DOI: <https://doi.org/10.1039/C0CE00975J>.
- [178] J. Moavi, F. Buazar, and M.H. Sayahi. *Sci. Rep.*, **11**:6296, 2021. DOI: <https://doi.org/10.1038/s41598-021-85832-z>.
- [179] M.T. Kiani, A. Ramazani, and S.Taghavi Fardood. *Appl. Organomet. Chem.*, **37**:e7053, 2023. DOI: <https://doi.org/10.1002/aoc.7053>.
- [180] M.B. Gawande, A.K. Rathi, P.S. Branco, T. Potewar, A. Velinho, I.D. Nogueira, A. Tolstogouzov, C.A.A. Ghumman, and O.M. Teodoro. *RSC Adv.*, **3**:3611–3617, 2013. DOI: <https://doi.org/10.1039/C2RA22511E>.
- [181] L. Moradi and Z. Ataei. *Green Chem. Lett. Rev.*, **10**:380–386, 2017. DOI: <https://doi.org/10.1080/17518253.2017.1390611>.
- [182] M. Kataria, S. Pramanik, M. Kumar, and V. Bhalla. *Chem. Commun.*, **51**:1483–1486, 2015. DOI: <https://doi.org/10.1039/C4CC09058F>.
- [183] S. Swami, N. Devi, A. Agarwala, V. Singh, and R. Shrivastava. *Tetrahedron Lett.*, **57**:1346–1350, 2016. DOI: <https://doi.org/10.1016/j.tetlet.2016.02.045>.
- [184] M. Abaszadeh, M. Seifi, and A. Asadipour. *Synth. React. Inorg. Met.-Org. Chem.*, **46**:512–517, 2016. DOI: <https://doi.org/10.1080/15533174.2014.988812>.
- [185] A. Ramazani, F. Moradnia, H. Aghahosseini, and I. Abdolmaleki. *Curr. Org. Chem.*, **21**:1612–1625, 2017. DOI: <https://doi.org/10.2174/1385272821666170420172606>.
- [186] H. Saeidian, Z. Mirjafary, E. Abdolmaleki, and F. Moradnia. *Synlett*, **24**:2127–2131, 2013. DOI: <https://doi.org/10.1055/s-0033-1339641>.
- [187] F. Moradnia, S. Taghavi Fardood, and A. Ramazani. *Appl. Organomet. Chem.*, page e7315, 2023. DOI: <https://doi.org/10.1002/aoc.7315>.
- [188] C. Hulme and V. Gore. *Curr. Med. Chem.*, **10**:51–80, 2003. DOI: <https://doi.org/10.2174/09298670333368600>.
- [189] S. Taghavi Fardood, A. Ramazani, M. Ayubi, F. Moradnia, S. Abdpour, and R. Forootan. *Chem. Method.*, **3**:519–525, 2019. DOI: <https://doi.org/10.33945/SAMI/CHEMM.2019.5.1>.
- [190] G. Jayakumar, A.A. Irudayaraj, and A.D. Raj. *Mater. Today: Proc.*, **4**:11690–11695, 2017. DOI: <https://doi.org/10.1016/j.matpr.2017.09.083>.
- [191] A.J. Christy and M. Umadevi. *Mater. Res. Bull.*, **48**:4248–4254, 2013. DOI: <https://doi.org/10.1016/j.materresbull.2013.06.072>.
- [192] K. Maniammal, G. Madhu, and V. Biju. *Nano-Struct. Nano-Objects*, **16**:266–275, 2018. DOI: <https://doi.org/10.1016/j.nanoso.2018.07.007>.
- [193] K. Motevalli, Z. Zarghami, and M. Panahi-Kalamuei. *J. Mater. Sci. Mater. Electron.*, **27**:4794–4799, 2016. DOI: <https://doi.org/10.1007/s10854-016-4360-5>.
- [194] Z. Qing, L. Haixia, L. Huali, L. Yu, Z. Huayong, and L. Tianduo. *Appl. Surf. Sci.*, **328**:525–530, 2015. DOI: <https://doi.org/10.1016/j.apsusc.2014.12.077>.



- [195] S. Rakshit, S. Chall, S.S. Mati, A. Roychowdhury, S. Moulik, and S.C. Bhattacharya. *RSC Adv.*, **3**:6106–6116, 2013. DOI: <https://doi.org/10.1039/C3RA21978J>.
- [196] M. Ranjbar, M.A. Taher, and A. Sam. *J. Mater. Sci. Mater. Electron.*, **26**:8029–8034, 2015. DOI: <https://doi.org/10.1007/s10854-015-3458-5>.
- [197] Z. Sabouri, A. Akbari, H.A. Hosseini, and M. Darroudi. *J. Mol. Struct.*, **1173**:931–936, 2018. DOI: <https://doi.org/10.1016/j.molstruc.2018.07.063>.
- [198] X. Wan, M. Yuan, S.-l Tie, and S. Lan. *Appl. Surf. Sci.*, **277**:40–46, 2013. DOI: <https://doi.org/10.1016/j.apsusc.2013.03.126>.
- [199] X. Wang, H. Mao, and Y. Shan. *RSC Adv.*, **4**:35614–35619, 2014. DOI: <https://doi.org/10.1039/C4RA04688A>.
- [200] Y. Wang, F. Zhang, L. Wei, G. Li, and W. Zhang. *Physica B*, **457**:194–197, 2015. DOI: <https://doi.org/10.1016/j.physb.2014.10.014>.
- [201] O. Baytar, A. Ekinci, Ö. Şahin, and S. Kutluay. *Mater. Sci. Eng., B*, **296**:116704, 2023. DOI: <https://doi.org/10.1016/j.mseb.2023.116704>.
- [202] K.S.G. Jagan, S. Surendhiran, S. Savitha, K.S. Balu, M. Karthick, T.M. Naren Vidarth, A. Karthik, B. Kalpana, and R. Senthilmurugan. *Inorg. Chem. Commun.*, **151**:110618, 2023. DOI: <https://doi.org/10.1016/j.inoche.2023.110618>.
- [203] N. Sundaresan, S. Ravichandran, and I. kaliappan. *Inorg. Chem. Commun.*, **150**:110489, 2023. DOI: <https://doi.org/10.1016/j.inoche.2023.110489>.
- [204] T.L. Pushparaj, E.F.I. Raj, E.F.I. Rani, and M.C. Thanu. *Appl. Organomet. Chem.*, **37**:e7285, 2023. DOI: <https://doi.org/10.1002/aoc.7285>.
- [205] K. Motene, L. Mahlaule-Glory, N. Ngoepe, M. Mathipa, and N. Hintsho-Mbita. *Int. J. Environ. Anal. Chem.*, **103**:1107–1122, 2023. DOI: <https://doi.org/10.1080/03067319.2020.1869730>.
- [206] A.L. Gajengi and B.M. Bhanage. *Catal. Lett.*, **146**:1341–1347, 2016. DOI: <https://doi.org/10.1007/s10562-016-1762-1>.
- [207] J.A. Tanna, R.G. Chaudhary, N.V. Gandhare, A.R. Rai, and H.D. Juneja. *Int. J. Scientific Eng. Res.*, **6**:93–99, 2015. DOI: <https://doi.org/10.13140/RG.2.1.2036.0088>.
- [208] H. Sachdeva, D. Dwivedi, R. Bhattacharjee, S. Khaturia, and R. Saroj. *J. Chem.*, **2013**:1–10, 2012. DOI: <https://doi.org/10.1155/2013/606259>.
- [209] P. Khyaliya, A.P. Devi, S. Kumar, R. Kant, and K.L. Ameta. *Chem. Biol. Lett.*, **7**:55–62, 2020.
- [210] J. Safaei-Ghomi and S. Paymard-Samani. *Chem. Heterocycl. Compd.*, **50**:1567–1574, 2015. DOI: <https://doi.org/10.1007/s10593-014-1625-x>.
- [211] M. Khashaei, L. Kafi-Ahmadi, S. Khademinia, A. Poursattar Marjani, and E. Nozad. *Sci. Rep.*, **12**:8585, 2022. DOI: <https://doi.org/10.1038/s41598-022-12589-4>.